journal of the mechanical behavior of biomedical materials 113 (2021) 104149

Contents lists available at ScienceDirect

Journal of the Mechanical Behavior of Biomedical Materials

journal homepage: http://www.elsevier.com/locate/jmbbm

Domain focused and residue focused phosphorylation effect on tau protein: A molecular dynamics simulation study

Md Ishak Khan, Fuad Hasan, Khandakar Abu Hasan Al Mahmud, Ashfaq Adnan *

Department of Mechanical and Aerospace Engineering, University of Texas at Arlington, Arlington, TX, 76019, USA

A B S T R A C T

Phosphorylation has been hypothesized to alter the ability of tau protein to bind with microtubules (MT), and pathological level of phosphorylation can incorporate formation of Paired Helical Filaments (PHF) in affected tau. Study of the effect of phosphorylation on different domains of tau (projection domain, microtubule binding sites and N-terminus tail) is important to obtain insight about tau neuropathology. In an earlier study, we have already obtained the mechanical properties and behavior of single tau and dimerized tau and observed tau-MT interaction for normal level of phosphorylation. This study attempts to obtain insights on the effect of phosphorylation on different domains of tau, using molecular dynamics (MD) simulation with the aid of CHARMM force field under high strain rate. It also determines the effect of residue focused phosphorylation on tau-MT interaction and tau accumulation tendency. The results show that for single tau protein, unfolding stiffness does not differ significantly due to phosphorylation, but stretching stiffness can be much higher than the normally phosphorylated protein. For dimerized tau protein, the stretching required to separate the protein forming the dimer is similar for phosphorylation in individual domains but is significantly less in case of phosphorylation in all domains. For tau-MT interaction simulations, it is found that for normal phosphorylation, the tau separation from MT occurs at higher strain for phosphorylation in projection domain and N-terminus tail, and earlier for phosphorylation in all domains altogether than the normal phosphorylation state. The residue focused phosphorylation study also shows that tau separates earlier from MT and shows stronger accumulation tendency at the phosphorylated state, while preserving the highly stretchable and flexible characteristic of tau. This study provides important insight on mechanochemical phenomena relevant to traumatic brain injury (TBI) scenario, where the result of mechanical loading and posttranslational modification as well as conformation decides the mechanical behavior.

1. Introduction

Phosphorylation has been associated with traumatic brain injury (TBI), dementia, Alzheimer's disease (AD), formation of paired helical filaments (PHF) and neurofibrillary tangles (NFT) in tau and other neurodegenerations (Hawkins et al., 2013; Shultz et al., 2015). It can occur in different ways in tau, and while some modes can alter electrophoretic mobility of tau, some other modes cannot; and phosphorylation is correlated to AD PHF, causing cytoskeletal alterations (Baudier and Cole, 1987). Specifically, tau in AD brain is abnormally phosphorylated protein component of PHF (Grundke-Iqbal et al., 1986). Therefore, it has gained attention in the recent years in cytoskeletal modeling studies. In this section, we will discuss the effect of phosphorylation and dephosphorylation that incorporates significant structural and chemical changes to cytoskeletal components, especially on tau-MT interaction.

As tau protein is an intrinsically disordered protein (IDP), a brief introduction on IDP is relevant for this study (repeated in relevance, earlier discussed in our work on tau protein response under strict mechanical loading). Intrinsically disordered proteins (IDP) are special proteins involved in many different cell-signaling pathways within the cell. They have unique capabilities of performing different functions based on conformations that occur due to different post-translational modifications, different binding substrates (proteins, nucleic acids, fibers, etc.) and fewer of the order-promoting amino acids found within hydrophobic cores of proteins. These include tryptophan, cysteine, tyrosine, leucine, phenylalanine, isoleucine, and valine. On the other hand, the amino acid make-up of an IDP commonly includes an abundance of amino acids associated with disorder, including alanine, arginine, glycine, glutamine, serine, proline, glutamate, and lysine (Jorda et al., 2010). In recent years, IDPs have been more prominent in biomedical research in an effort to understand their variable roles. This paper discusses tau, which is heavily involved in Alzheimer's Disease (AD), but Parkinson's disease (alpha-synuclein), Amyotrophic Lateral Sclerosis (superoxide dismutase-1), and Huntington's Disease (poly--glutamine gene products) are also caused by IDPs (Uversky, 2010). Without stable conformations and singular, defined functions, IDPs are prone to aggregation and once aggregated, burden the cell's degradation machinery.

* Corresponding author.
E-mail address: aadnan@uta.edu (A. Adnan).

https://doi.org/10.1016/j.jmbbm.2020.104149
Received 29 August 2020; Received in revised form 13 October 2020; Accepted 17 October 2020
Available online 21 October 2020

After clarification on IDPs, we can move on to the specific introduction on phosphorylation effect on such proteins. Phosphorylation means attachment of a phosphoryl group to a molecule, and it has been considered important in protein functionalities, along with its counterpart named dephosphorylation. Phosphorylation has been shown to affect the activity of tau in vitro and microtubule associated protein activities in vivo, and it can be obtained by several protein kinases (Lindwall and Cole, 1984). Identification of the phosphorylated sites in abnormally phosphorylated protein samples is the approach to identify the respective kinases or phosphatases involved (Goedert et al., 1989). Cause of phosphorylation has been hypothesized as the function of several kinases and phosphatases (Churcher, 2006; Mazanetz and Fischer, 2007). Numerous studies have suggested that phosphorylated taus are less effective than non-phosphorylated ones on MT polymerization (Biernat et al., 1993; Bramblett et al., 1993; Cleveland et al., 1977). It has also been found as a developmentally regulated phenomenon (Dudek and Johnson, 1995; Mawal-Dewan et al., 1994; Ono et al., 1995), or in elaboration, we can say that extent of phosphorylation in fetal tau can be compared to that of PHF tau from AD PHF (Kenessey and Yen, 1993).

More importantly, it has been hypothesized to alter the ability of tau to bind microtubules (Buée et al., 2000), though the specific mechanism of phosphorylation in this regard is uncertain. Electron micrography study shows that dephosphorylated tau can facilitate rapid polymerization of microtubules (Lindwall and Cole, 1984), and also that partially purified microtubules contain kinase which is capable of re-phosphorylation of tau. The current conjecture is that the role of more than one enzymes (candidate kinases) might be related to phosphorylation and alteration of MT binding, and that kinase inhibitors can control the process of hyperphosphorylation, although existent review work admits that roles of MT associated kinases and phosphatases are yet to be fully described (Billingsley and Kincaid, 1997), and it is not clear how many of them participate in tau phosphorylation in vivo (Buée et al., 2000). However, some specific studies have marked some kinases as related to controlling phosphorylation, such as GSK3, CDK5, MARK, etc. (Ferrer et al., 2005; Mazanetz and Fischer, 2007; Noble et al., 2005). Some studies on bovine and rat brains have shown that Calcium/calmodulin (CaM) dependent protein kinases can phosphorylate taus which is similar to AD lesions (Mandelkow and Mandelkow, 1998).

Phosphorylation "level" has been hypothesized as an important marker of tau pathology, because it is at different levels in normal (or healthy) tau, fetal tau, adult tau and AD affected brains (Brandt and Lee, 1993), and in general is related to the detachment from MTs, leading to changes in MT dynamics (Ballatore et al., 2007). Tau protein itself is a biomarker of AD, and both total and p-taus are increased in such disorders, as suggested by CSF studies (Sjögren et al., 2001). Experimentally it is found that levels of normal tau is significantly reduced in brain supernate from AD cases, or in other words, abnormally phosphorylated taus are increased in pathological scenarios (Khatoon et al., 1994; Köpke et al., 1993). Abnormal phosphorylation has been related to PHFs and AD and other neurodegenerative diseases, and therefore has obtained focus (Selkoe, 1991). However, there are some conflicting results in existence, which suggest that PHFs can be formed in a phosphorylation-independent manner also (Goedert et al., 1996). This "developmental regulation" aspect of phosphorylation is to be given proper attention, as different states of phosphorylation are observed in fetal and adult tau, and AD-like state similar to the fetal tau (Watanabe et al., 1993).

There have been separate studies on tau structure, which suggest that phosphorylation level plays a critical role to distinguish healthy tau from pathological tau (Becker and Przybylski, 2007), and it also has been hypothesized to alter the ability of tau to bind MTs as well as other functionalities (Hanger et al., 2009). Earlier Monte Carlo simulation study that has attempted to find out the threshold of tau pathology suggested that numerous candidate amino acids can be phosphorylated, but under pathological conditions around 7 of them are actually phosphorylated (Jho et al., 2010). The abnormally phosphorylated tau proteins are 3–4 times more phosphorylated than the normal ones, and around 2 sites per mole of tau protein can be phosphorylated in normal condition (Kenessey and Yen, 1993). Recently, cryo-EM technology has been able to obtain 3-4Å resolution image of paired helical filaments (PHF) in AD affected brains (Fitzpatrick et al., 2017), which is directly related to abnormal phosphorylation in tau. Total tau vs p-tau studies, in order to find CSF biomarkers for diagnosis of AD, have been plenty, and in general suggested that p-tau is higher in AD affected brains (Mulder et al., 2010). Differential diagnosis of AD with cerebrospinal fluid (CSF) levels of tau phosphorylated at Thr-231 showed that the level is significantly higher in AD affected samples (Buerger et al., 2002). Another study also showed that CSF level of tau phosphorylated at Ser-396 and Ser-404 can be diagnostic marker of AD (Hu et al., 2002). Also, separate CSF study on patients suggested in a similar way, that phosphorylated tau (p-tau) level is higher in AD brain than normal control group (Kandimalla et al., 2013). Therapeutic approaches targeting tau have recently focused on inhibiting tau fibril formation or dissolution of pre-existing aggregates, and thus preventing aberrantly phosphorylated and/or misfolded tau from forming more organized aggregates (Pickhardt et al., 2005). It is also believed that dephosphorylation is related to regaining MT functions and structural integrity (Ballatore et al., 2007). Furthermore, some phosphorylation related studies using separate phosphorylation dependent antibodies show that severity of the tau pathology (formation of PHF and NFT) can be related to this process in AD affected brains (Mandelkow et al., 1995).

Also, there are separate studies in existent literature that focus on phosphorylation of specific residue (such as Ser-262), which show that certain serine phosphorylation can strongly reduce binding of tau to MTs (Biernat et al., 1993) (Biernat et al.). Early studies showed that different serine residue such as Ser-199, Ser-202, Ser-409, Ser-396 and threonine residues such as Thr-231 are phosphorylated in NFTs (Götz et al., 1995). Phosphorylation in Ser-202 has been suggested to recapitulate phosphorylation in developmental stage (Goedert et al., 1993). Thr-181 has been related to AD in separate researches, where phosphorylated Thr-181 quantification has been analyzed (Haense et al., 2008; Ravaglia et al., 2008; Vanmechelen et al., 2000). A review work has also found hyperphosphorylation in PHFs in general (Götz et al., 1995). In vivo experiments has shown that green fluorescent protein (GFP) tau attaches with MT in a phosphorylation-dependent manner (Samsonov et al., 2004). Critical site-based phosphorylation (such as in Ser-262, Thr-231, Ser-396) studies show that it can reduce MT binding and form aggregation of tau, and also can be developmentally regulated (Biernat et al., 1993; Bramblett et al., 1993). Quantification of binding of MT with tau is determined by the stoichiometry, or number of tubulin dimer attached to tau in phosphorylated state – the results of which suggested that phosphorylation can significantly reduce the stoichiometry, and creating mutated isoform by switching Ser-262 with an Alanine residue showed less sensitivity to phosphorylation, making it an important regarding tau-MT interaction. These studies also strengthen the argument that the residues can be phosphorylated by activity of more than one kinase and assert that although phosphorylation in many candidate amino acids (AA) is possible, certain phosphorylated residues can have major effect on MT binding.

However, these studies also admit that the causal relationship between phosphorylation in specific site and reduced binding ability to MT, or pathology is debatable. Studies on monoclonal antibodies have been manifold, because it has been found that PHF tau reacts with certain antibodies in a phosphorylation-dependent manner, and these studies have suggested that phosphorylation in Ser-199 and/or Ser-202 might be related to switch of normal tau to AD-like state tau in a reversible manner (Biernat et al., 1992). Although it might seem that phosphorylation in single sites can lead to decreased level of MT binding, this phenomenon is thought as insufficient to eliminate MT binding altogether (Seubert et al., 1995). Also, phosphorylation mechanism can be more complex than depicted in the above discussion focusing on the

Table 1
Selection of phosphorylation sites in tau protein based on earlier studies.

Critical Phosphorylation Site	Reference No.
Ser199, Ser202, Ser396, Ser 409, Thr231	(Biernat et al., 1992; Mandelkow and Mandelkow, 1998; Mandelkow et al., 1995; Pickhardt et al., 2005; Santarella et al., 2004; Trinczek et al., 1995)
Thr181	(Biernat et al., 1992; Fitzpatrick et al., 2017; Goedert et al, 1989, 1992; Götz et al., 1995)
Thr231	(Buerger et al., 2002; Haense et al., 2008)
Ser396, Ser 404	(Bramblett et al., 1993; Hu et al., 2002; Kenessey and Yen, 1993)
Ser199, Ser202, Ser262	Trinczek et al. (1995)
Ser199, Ser202, Ser 205, Ser 235, Ser262, Ser 356, Thr212, Thr231	(Biernat et al., 1993; Goedert et al., 1993; Iqbal et al., 1989; Seubert et al., 1995)
R1-R2 inter-region	Buée et al. (2000)

effect of phosphorylation of specific sites, because in abnormal condition (PHF tau), clustering can occur to the sites, giving multiple phosphorylated peptides with possible mutually exclusive combinations of phosphorylation (Goedert et al., 1992). As there are numerous putative phosphorylation sites in tau, and in AD more than 30 sites are phosphorylated which are determined by mass spectrometry, identification of critical sites (which are involved in converting normal tau to a pathological one) is difficult. However, some studies have shown that Ser-262, Thr-231 and Ser-235 inhibits the binding to MT by ~35%, ~25% and ~10% respectively (Iqbal et al., 1989). Other studies suggest that candidate critical sites can be Ser-199/202/205, Thr-212, Thr-231/Ser-235, Ser-262/356 and Ser-404, while Thr-231, Ser-396 and Ser-422 can promote self-assembly of tau into filaments (Alonso et al., 2004) (quantification comes from phosphate per mole of tau studies, which suggests that 4–6 phosphates/mol of protein indicates pathology). The residue-specific studies suggest that MT binding domain and its vicinity are the most important candidates to examine the effect of phosphorylation, especially the R1-R2 inter-region, which is also the most potent region for MT polymerization (Goode and Feinstein, 1994; Panda et al., 1995). Site-specific phosphorylation can lead to loss of MT binding, and weakening of the neuronal cytoskeleton (Mandelkow et al., 1995). Specific domain-focused studies have targeted MT binding site residues to observe the phosphorylation effects (Scott et al., 1991). However, such studies are not conclusive, because the structural integration and disintegration mechanism is highly complex and modulated by other parameters than tau phosphorylation (Avila, 1990). Dephosphorylation has been found to restore the ability of PHF to bind, but it is not clear how phosphorylation sites outside the MT binding region can regulate tau-MT interactions (Garver et al., 1996).

We have already mentioned computational studies performed on tau-MT interaction as well. The other aspects of Monte Carlo simulation of tau-MT showed that due to charged nature of MT, electrostatic interaction is important to analyze their behavior, and while amino acids in tail domain of tau stay mostly apart from the MT surface, in bulk solution dephosphorylated taus are separated due to coulomb repulsion between similarly charged isoforms, and moderate phosphorylation can decrease average intermolecular distance between dephosphorylated and phosphorylated taus, leading to their overlap (Jho et al., 2010).

Based on the discussion above, phosphorylation can be considered as a biomarker for decreasing tau-MT bonding, but deeper investigations are still needed on the parameters and mechanisms that control phosphorylation. There are different mechanisms, such as O-glycosylation which are hypothesized to negatively regulate phosphorylation, and believed to be involved in AD (Liu et al., 2004; Yuzwa et al., 2008). Such investigations have suggested that reduced O-glycosylation can lead to hyperphosphorylation and eventually, the disorders we have mentioned above.

There are certain limitations in the studies on phosphorylation effect, although numerous studies exist in literature. To mention a few, the studies cannot clarify the mechanisms of the effect of phosphorylation on residues outside MT binding region, they cannot conclusively answer the zone-based phosphorylation effect and pathological threshold of tau protein, and they cannot form any specific causal reason between phosphorylation in specific sites and reduced tau-MT interaction. Furthermore, similar phosphorylation state can be observed in normal and diseased taus – which clearly indicate that phosphorylation is not a stand-alone parameter to determine pathology. This study attempts to answer certain questions which were incompletely or not answered in earlier studies on domain-focused or residue-focused tau studies, such as how the mechanical stiffness of single tau is altered due to phosphorylation in different domains, how the required stretch for separation in dimerized tau is affected by this phenomenon, or how the tau-MT interaction is changed (tau-MT interaction studies have proposed several probable mechanism including hyperphosphorylation in specific residues leading to decreased tau-MT binding, but inconclusively).

The MD simulations in the current study are designed accordingly: for single tau, we have obtained the secondary structure from i-TASSER (Zhang, 2008) predictor software and applied phosphorylation on relevant sites using CHARMM-GUI (Jo et al., 2008) to imitate phosphorylated condition. For domain focused phosphorylation, we have applied phosphorylation in different domains, while for residue focused phosphorylation, we have applied phosphorylation in specific residues (details in the "Method" section). For dimerized tau, we have made the models with overlapped projection domains as depicted by Rosenberg et al. (2008). For tau-MT interaction, we have used Chau et al. proposals of interaction, where tau can interact with one or both subunits of MT (Chau et al., 1998). We have applied phosphorylation to the dimerized and tau-MT models in the similar manner as single tau models. In the results and discussions section, we discuss on the tensile tests performed on all the models in detail.

2. Method

Tau protein has three domains in its structure: projection domain, MT binding domain, and tail domain. The projection domain of one tau creates electrostatic zipper bond with the projection domain of another tau – resulting in dimerized tau (Rosenberg et al., 2008). Furthermore, tau proteins attach themselves onto the surface of MT through the MT binding domain (Chau et al., 1998). Therefore, while designing tensile tests, there are three scenarios to be considered: first, single tau projection domain unfolding and stretching needs to be differentiated based on the applied strain rate; second, dimerized tau separation strain needs to be determined, and third, the tau-MT separation stretch needs to be determined. These specific scenarios are relevant to TBI scenario, as while susceptible to TBI, single tau projection domain gets significantly stretched, dimerized tau proteins become vulnerable to stress development in their overlapped projection domain areas, and tau gets stretched which leads to separation from MT surface. It is also important to differentiate their mechanical behavior according to their phosphorylated states. Therefore, in single tensile tests, we have stretched single tau projection domain while keeping the MT binding region fixed. In dimerized tau system, we have pulled the MT binding domain of one tau protein while keeping the MT binding domain of another tau. In tau-MT system, we have pulled the tau projection domain from MT surface, and determined at what strain the MT binding domain of the tau gets separated from the MT surface. At the end of the Method section, Table 2 shows the simulation box sizes used in this study.

By going through the recent computational approaches on intrinsically disordered proteins (IDPs), we have found that recent years have observed significant improvement in computational studies by using predicted structure. Notable examples are electrostatic study (Castro et al., 2019) and aggregation behavior study on tau (Battisti et al., 2012). The method used here is the similar to our earlier work on single tau, dimerized tau and tau-MT interaction models, except that we have incorporated new models with phosphorylation in different domains of

Table 2
Simulation Box Sizes and Setup Used in this Study.

Phosphorylation State	System	Simulation box size (nm x nm x nm)	Setup
Domain Phosphorylation	Single Tau	30 × 12 x 12	MT binding site is fixed and projection domain is pulled
	Dimerized Tau	200 × 20 x 15	MT binding site of one protein is fixed, MT binding site of another protein is pulled
	Tau-MT	200 × 20 x 15	Upper and lower layers of MT are fixed, tau projection domain is pulled
Residue Phosphorylation	Tau-MT	182 × 39 × 33	Upper and lower layers of MT are fixed, tau projection domain is pulled
	Tau Accumulation: 2 tau system	40 × 20 x 15	1ns equilibration
	Tau Accumulation: 3 tau system	40 × 20 x 15	1ns equilibration
	Tau Accumulation: 4 tau system	40 × 20 x 20	1ns equilibration
	Tau Accumulation: 6 tau system	40 × 20 x 20	1ns equilibration

tau to observe how chemical effects withstand extreme mechanical loading. It is already substantiated by recent review study that such molecular level study on mechanical behavior is required to obtain a comprehensive insight regarding tau (Khan et al., 2020).

In the current study, the tau protein structure is obtained from i-TASSER predictor software. We have used the model with the C score of −0.03 (the C score is determined based on significance of threading template alignments and the convergence parameters of the structure assembly simulations) which we have assumed satisfactory for an IDP. We have used the quick-MD simulator module from CHARMM-GUI for applying phosphorylation. Phosphorylation was applied to these Serine (SER) residues for domain focused phosphorylation: a. for projection domain: 46, 56, 61, 64, 68, 113, 129, 131, 137, 184; b. for MT binding sites: 258, 262, 285, 289, 293, 305, 316, 320, 324, 341; and c. for N-terminus tail: 396, 400, 404, 409, 412, 413, 416, 422, 433, 435. Finally, for the set with phosphorylation in all domains, we mean that all the SER residues mentioned above are phosphorylated simultaneously. In case of residue focused phosphorylation, we have selected 7 residues which have been found at phosphorylated state widely in case of neuropathology such as formation of PHF or AD. These selected residues consist of six serine (SER) residues: 199, 202, 262, 396, 404, 409, and Threonine (THR) residue 231. The selection was made according to earlier studies, the reference list of which is shown in Table 1. We have focused on the residues which are found to have decreased tau-MT bonding in one or more studies.

The dimerized model was created by using UCSF Chimera (Pettersen et al., 2004), in which we have overlapped the projection domains of two identical tau proteins. We have used implicit solvent technique of CHARMM in LAMMPS (pair_style lj/charmm/coul/charmm/implicit command) for the tensile tests of dimerized tau and tau-MT interaction, which facilitates a bigger box size, faster calculation and therefore, convenient observation of the protein systems we have built, at the cost of more realistic scenario of explicit water molecules, which would be computationally demanding at our required box sizes. The implicit solvent mechanism computes with a modification of adding an extra r^{-1} term for Coulombic energy calculation, which depicts a simpler calculation method for unsolvated biomolecules. The reader can find the relevance of using implicit solvent simulation for such cytoskeletal systems from the supplementary material of Wu et al. (Wu and Adnan, 2018).

For domain focused phosphorylation, the MT structure is obtained from the existing model built by Wells et al. (Wells and Aksimentiev, 2010). We have used the N system described in the paper, in which there are helically organized four subunits (two α, two β) and the same type of subunits are placed beside each other, each having one GTP or a GDP, along with one Mg^{2+} ion in the junction. The tau-MT interaction system was created by UCSF Chimera as well, where the tau binding sites are placed in close proximity of the MT binding sites as proposed by Chau et al. (1998). For residue focused phosphorylation, we have attached the MT binding sites of two different tau proteins on the MT surface, one being normal and the another phosphorylated at the 7 residues. The full MT structure is obtained by periodically repeating the helical structure along the length direction, creating a virtually infinite MT. In the accumulation test, we have created four (4) systems: 2 tau system, 3 tau system, 4 tau system, and 6 tau system. The 3 tau system is the reference system, while 2 tau system is created by removing the second protein from the 3 tau system, 4 tau system is created by offsetting protein 1 at 40 Å distance in z-direction, 6 tau system is created by offsetting protein 1, 2, and 3 at 40 Å distance in z-direction. In reference 3 tau system, the tau proteins are placed in random orientation, in the vicinity of each other and in presence of explicit water molecules, and then equilibrated for 1 ns at 310 K NVT ensemble. The equilibration setting is the same for 2, 4, and 6 tau systems.

For the tensile tests, with periodic boundary conditions in all three directions, we have equilibrated the structures for all cases (single tau, dimerized tau and tau-MT) for 100ps to minimize the potential energy at a targeted temperature of 310 K. Single tau, dimerized tau and tau-MT contained ~6400, ~12,800 and ~33,000 atoms respectively (the exact number of atoms varied according to the level of phosphorylation). The LJ potentials are used with inner and outer cutoff of 10 Å and 12 Å, respectively.

We have used CHARMM36 (Best et al., 2012; Brooks et al., 2009; MacKerell et al., 1998) potential parameters with appropriate CMAP corrections (Buck et al., 2006) for all the simulations. Potentials for GDP and GTP are taken from that of ADP and ATP respectively (Wells and Aksimentiev, 2010). The equilibration was performed in NVT canonical ensemble, with the temperature damping parameter of 100fs.

Tensile tests are performed in different manners for domain focused and residue focused phosphorylation. In the tensile test on single tau, we have fixed the MT binding domain and pulled the projection domain along x axis. For dimerized tau, we have fixed the MT binding domain of one protein and pulled away the MT binding domain of another protein along x axis. For tau-MT, we have fixed the microtubule subunits (the portions that are opposite of the tau binding sites on them) and pulled away the tau protein. Tau-MT tensile tests are done at high strain rate ($2 \times 10^9\ s^{-1}$). However, for residue focused phosphorylation, the upper and lower layers of the periodic MT structure were fixed, while few projection domain atoms of the attached tau proteins were pulled at two different strain rates ($10^9\ s^{-1}$ and $2 \times 10^9\ s^{-1}$). For the tau accumulation test, only 1ns equilibration was assumed sufficient to observe. The high strain rate on neural cytoskeletal components are relevant to TBI scenario, which we attempt to focus on particularly (Wu and Adnan, 2018).

LAMMPS allows to calculate the force on a group of atoms along with the displacement with convenience. Furthermore, stress-strain plots are obtained by the per-atom stress calculation and summation in LAMMPS. However, as the output is in (pressure x volume) unit, we must divide the obtained stress value by the volume of the protein (or certain portion of the protein). The general formulation used by stress per atom command is $P = (P_{xx} + P_{yy} + P_{zz})/(3xV)$, where P_{xx}, P_{yy} and P_{zz} is the summation of stress/atom value for all atoms in x, y, and z direction respectively, and V is the summation of volume of the atoms of the protein being considered. The approximated volume was obtained by Voronoi cell approximation, adapted from LAMMPS voro++ package (Rycroft, 2009). The strain is simply obtained by the displacement of the atoms from the initial position. All the tensile tests are performed in NVT ensemble, with 100fs temperature damping parameter. The

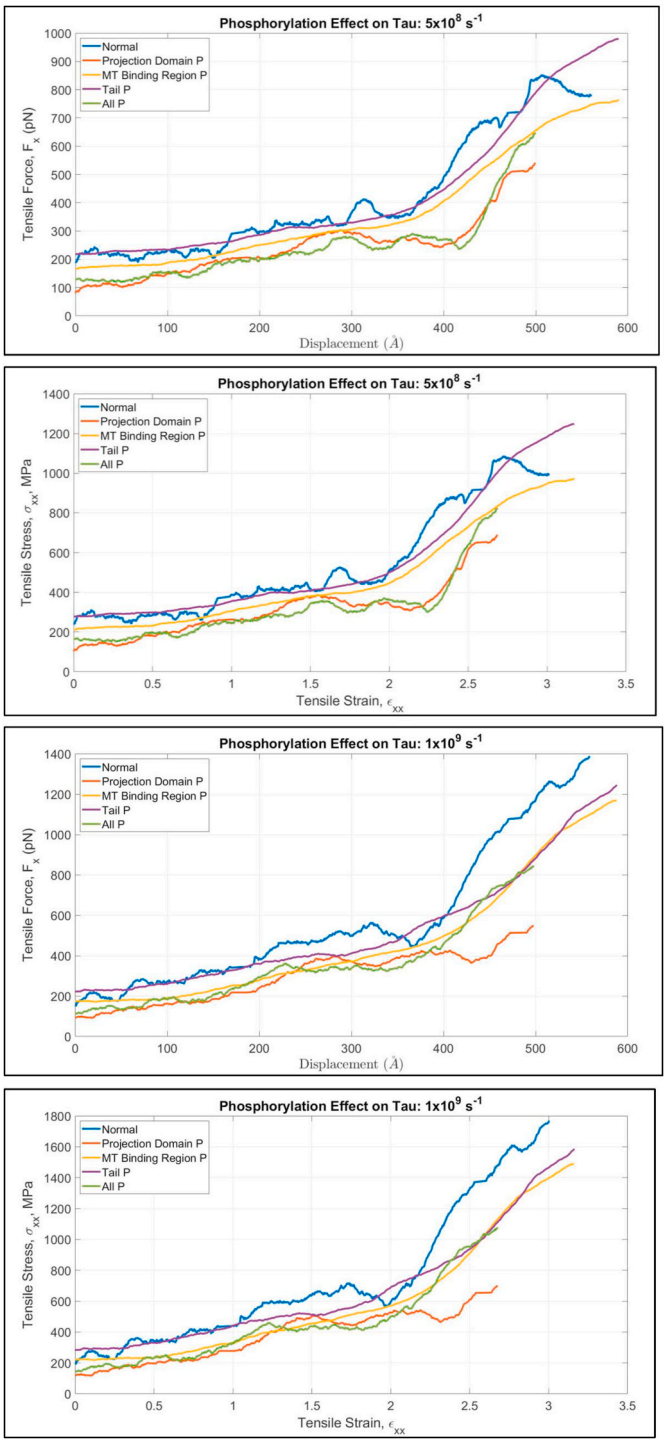

Fig. 1a. Force vs Displacement and Stress vs strain plot of single tau projection domain. Up to ~175% strain, tau protein keeps unfolding, and after that we see a sharp rise in the slope, suggesting the pure stretching of covalent bonds. We have obtained results for greater than 300% strain for most cases, but only up to ~268% strain is shown for all cases. i-ii) $5 \times 10^8 s^{-1}$, iii-iv) $1 \times 10^9 s^{-1}$. Data smoothened by using moving average.

visualizations of the tensile tests are carried out by OVITO software (Stukowski, 2010).

All the simulations were carried out by the STAMPEDE2 supercomputer of Texas Advanced Computing Center (TACC).

3. Results

3.1. Domain focused phosphorylation

3.1.1. Single tau unfolding and stretching

We have performed the tensile tests at high strain rates (5×10^8 s^{-1} and 1×10^9 s^{-1}). The MT binding region atoms are fixed, and first few atoms of the projection domain are pulled at –x direction. The calculated force-displacement and stress-strain graphs are shown in Fig. 1a. As we have already seen in our previous work, unfolding is followed by stretching of the covalent bonds, therefore we observe two distinct slopes in the graph. The stretching does not begin until the tau is highly unfolded (~200%), and that is followed by a combination of unfolding and stretching in the projection domain. We have calculated the unfolding stiffness from the linear fitting 0%–175% strain graphs, while the stretching stiffness is obtained from that of 200%–~268% strain graphs. Fig. 1b shows the different distinguishable stages of the tensile tests: unfolding and stretching. From our earlier work, we have shown that strain rate greatly affects the unfolding and stretching stiffness in both unfolding and stretching region. However, in the current work, Table 3 and Fig. 1 show that in the unfolding region the phosphorylation alters the stiffness dynamically. The results indicate that both at the unfolding and stretching regions, we have obtained different slopes for different phosphorylated domain. For phosphorylation in tail, we have obtained smallest slope in the unfolding region (<100 MPa). For normal, phosphorylation in MT binding sites and all domains, the stiffness is significantly higher in the stretching region. We can suggest that domain focused phosphorylation can dynamically affect the stiffness of single tau chain while unaffected by external parameters such as intervention of tau-MT interaction, and that we cannot predict a trend of increasing stiffness if we monotonously increase the number of phosphorylated sites by arbitrarily applying phosphorylation. However, we can attempt to predict the change of stiffness due to phosphorylation and strain rate dependency simultaneously, which is out of the scope of this manuscript. The estimated stiffness for both regions, however, are in reasonable range, according to our previous work on the effect of strain rate on tau protein and existent literature, and the randomness of our results strengthens the current hypothesis obtained from the literature that not only phosphorylation is responsible for the stiffness of the tau protein structure, but also other parameters may also be equally important.

3.1.2. Dimerized tau separation

We have attempted to observe the developed stress and possible sliding out of tau projection domain at high stretch, and the effect of phosphorylation on this phenomenon. We have fixed the MT binding site of one tau and pulled away the binding site of another tau. The force-displacement and stress-strain graphs (calculation procedure was similar to single tau) for the projection domain of the tau protein that has been pulled along the -x direction, at the strain rate of 2×10^9 s^{-1} were plotted in Fig. 2a (ii). Several sub-stages are observed as expected for the strain rate of 2×10^9 s^{-1} which are shown in Fig. 2b (we are referring to the protein with fixed MT binding region as protein 1, and the protein being pulled as protein 2): i. Unfolding of protein 2 (up to 163% strain), ii. Stretching of protein 2 (up to 257% strain), iii. Unfolding of protein 1 (up to 334% strain), iv. Stretching of protein 1 (up to 395% strain), v. Disentanglement of the overlapped projection domains of the tau proteins (up to 721% strain), vi. Sliding out or projection domain along with stretching (very fast, occurs at around 722%–758% strain region), and vii. Separation of proteins (~758% strain). For normal phosphorylation level, we have already observed that strain rate significantly affects the required stretch for separation. However, in this study, the phosphorylation in different domains hardly affected the separation stretch (~750%) except for the case of phosphorylation in all domains (~600%), while unfolding and stretching occur in the similar manner for all cases. We can conclude that although the existent studies

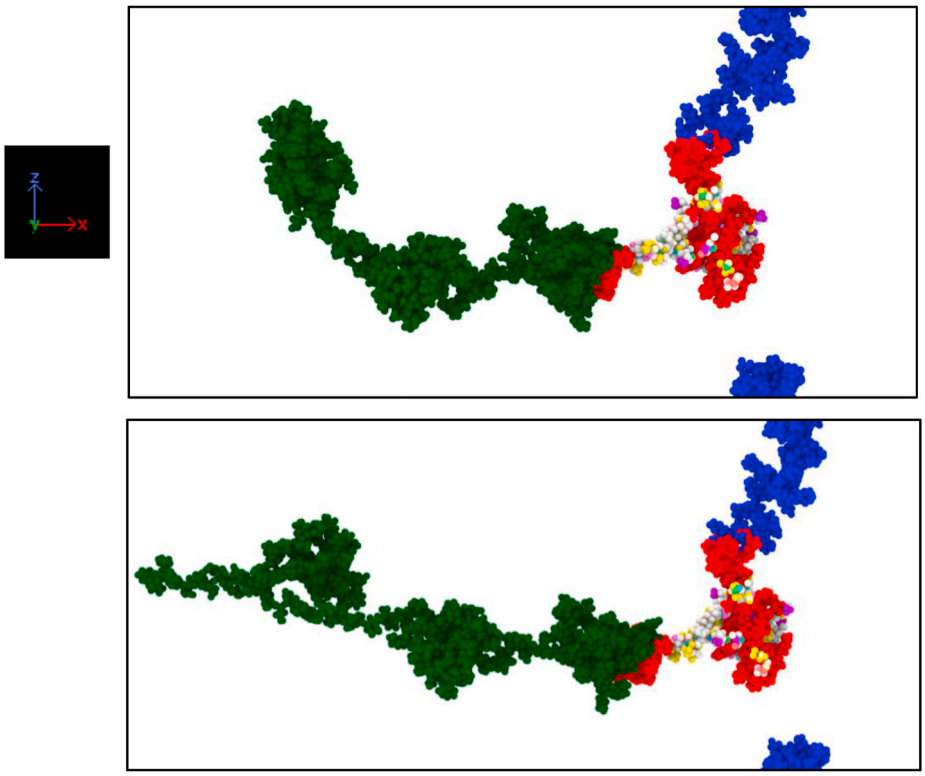

Fig. 1b. Different stages of the tensile test on single tau (normal phosphorylation, strain rate: $1 \times 10^9 s^{-1}$). i. Initial single tau structure (strain = 0%), ii. tau protein being unfolded due to pulling at $10^9\ s^{-1}$ (strain = 36%). Color legends: green: projection domain, red: MT binding region, blue: N terminus or tail, white: interrepeats between the MT binding regions. (For interpretation of the references to colour in this figure legend, the reader is referred to the Web version of this article.)

suggest that phosphorylation can promote accumulation of taus, it may not be reflected in separated dimerized tau, or domain focused phosphorylation can undermine the effect of phosphorylation on dimerized taus in an unpredictable manner, although the ability of tau for being highly stretched stays unaffected. In the Appendix, Figure A1 shows potential energy plots vs time, which suggests that although potential energy level is almost the same for all phosphorylation states, it significantly reduces at separation for all cases.

3.1.3. Tau-MT interaction

In our previous study, we have already shown the tau-MT interaction for normal phosphorylation, and that tau-MT bonding is stronger than MT subunit bonding. In this study, we perform similar tensile tests in high strain rate ($2 \times 10^9\ s^{-1}$) for domain focused phosphorylation. We observe different phenomena for phosphorylation at different domains, although the unfolding and stretching due to the pulling force are similar for all cases. The observations are summarized in Table 4. For all cases, we have observed expected tau protein unfolding followed by stretching. For normal phosphorylation, we observe vigorous stretching of MT binding site before separation from MT surface at the strain of 1125%. For phosphorylation in projection domain and tail, we observe similar stretching and separation at higher strain (1330%). For phosphorylation in all domains, we observe early separation, at 918%. However, the observation for phosphorylation in MT binding sites is quite different, we see that the MT binding region gets stretched significantly along with the MT tubulin surface, but does not separate, although we have continued the simulation for up to 2000% strain. It is to be noted that we have considered tau as separated from MT when the MT binding region of tau is completely separated from the MT surface. Fig. 3a(ii) and 3b shows the stress-strain graphs and the observed stages in the simulation. In the Appendix, Figure A2 shows the potential energy trend, which shows that potential energy takes a sharp decrease at separation for all cases.

Table 3
Unfolding stiffness and stretching stiffness of single tau for phosphorylation in different domains.

Strain Rate	$5 \times 10^8 s^{-1}$		$1 \times 10^9 s^{-1}$	
Phosphorylation Domain	Unfolding Stiffness (MPa)	Stretching Stiffness (MPa)	Unfolding Stiffness (MPa)	Stretching Stiffness (MPa)
Normal	129	549	285	1198
Projection Domain	144	442	227	317
MT Binding Sites	128	520	191	1050
Tail	97	731	179	890
All Domains	113	857	175	962

3.2. Residue focused phosphorylation

3.2.1. Tau-MT interaction: normal vs phosphorylated tau

The domain focused phosphorylation simulations have shown that we cannot establish a definite trend of the change of mechanical properties according to the phosphorylation at different domains of tau. Furthermore, it is possible that residue focused phosphorylation can provide more insight about the effect of phosphorylation. Therefore, we have performed another set of simulation by attaching one normal and one phosphorylated tau (phosphorylated in seven selected sites) on the same MT surface in order to understand which one is prone to separate earlier under the application of the same strain rate. We have pulled the tau projection domain at two different strain rates ($10^9 s^{-1}$ and $2 \times 10^9 s^{-1}$). In both cases, we have observed that the phosphorylated tau separates from the MT surface earlier than the normal tau (at ~90% less strain for both cases). The effect of strain rate is important for this study, as we have observed that at lower strain rate the separation occurs at higher strain, that is, high strain rate tends to separate the tau protein

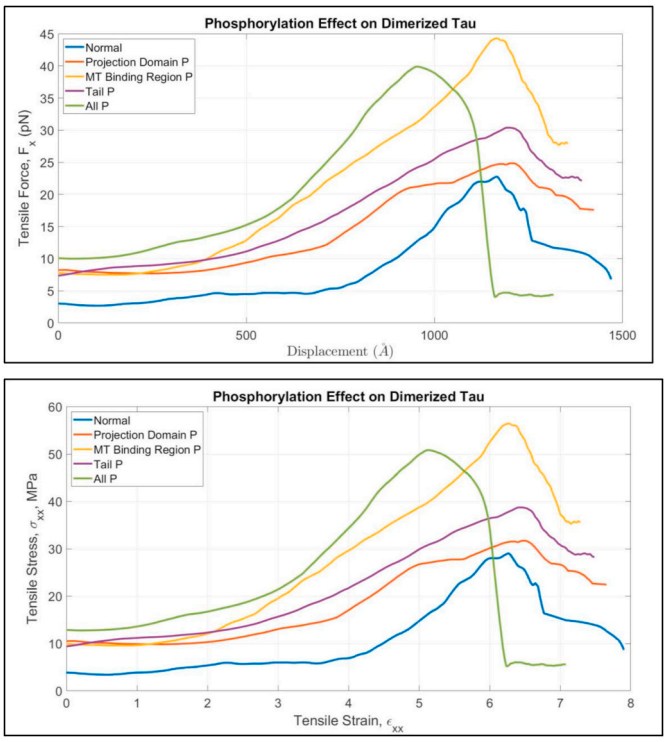

Fig. 2a. i. Force-Displacement and ii. Stress-strain curve of protein 2 projection domain for phosphorylation in different domains (strain rate: $2 \times 10^9 s^{-1}$). There are several stages observed before complete separation of dimerized tau: such as unfolding of protein 2, stretching of protein 2, unfolding of protein 1, stretching of protein 1, disentanglement of the overlapped projection domains along with stretching and finally, complete separation. Complete separation occurs at almost same strain for all the cases (~750%), except for phosphorylation in all domains simultaneously (~600%). Data smoothened by using moving average.

from the MT surface earlier, and at lower strain rate, the tau is able to stay attached with the MT surface for 20–40% more strain, depending on the strain rate, which is consistent with the results of our earlier work on tau-MT interaction. The observation is also compatible with earlier studies which suggested that phosphorylation significantly decreases tau-MT bonding (refer to Table 1 in the Method section). Additionally, this study further highlights the highly stretchable characteristic of tau and strong tau-MT bond, even at phosphorylated state. Fig. 4a shows the stress vs strain graph of the tau projection domain for the two strain rates. Fig. 4b shows the stages of tau-MT interaction in our simulation at the strain rate of $2 \times 10^9 s^{-1}$. Similar to the tau-MT interaction study in the first portion of the manuscript, tau is considered to be separated from MT when the MT binding region is completely separated from MT surface. Fig. 4a and b shows the force vs displacement and stress vs strain graphs for four sets of simulation, and observable stages up to separation, respectively. In the Appendix, Figure A3 shows the potential energy trend for the four sets, which suggests that potential energy decreases significantly at separation, and potential energy is significantly less at phosphorylated state than at normal state. Moreover, they are of close values irrespective of applied strain rate. The observation agrees to previous findings that phosphorylation alone cannot signify the stability of tau-MT system, and even at selectively phosphorylated state, the system can be more stable than at normal state.

3.2.2. Tau accumulation test

From the existent literature we already know that formation of PHF and tau accumulation are biomarkers of neuropathology, which are highly dependent on phosphorylation. As a part of residue based phosphorylation simulations, we have placed two, three, four, and six tau proteins in the simulation box in presence of explicit water molecules, minimized the potential energy and equilibrated at 310 K for 1ns in order to observe possible difference in tau accumulation for normal and phosphorylated cases. Although the potential energy graphs are similar for both normal and phosphorylated cases of all systems (refer to the Appendix, Figure A4-A7), we have observed that the normal taus did not accumulate throughout the simulation, while the phosphorylated ones shown distinguishable tendency to decrease the distance between each other. We admit that 1ns is very small timescale for observing total accumulation. Therefore, in order to quantify the decrement of the distances between the tau proteins, we have calculated the relative distance between the mass centers of the projection domains of the tau proteins throughout the simulation, and the differences between the coordinates depict how much they have come closer (or got further away) during the simulation. The calculation is focused on the projection domains of the tau proteins, as dimerization or polymerization occurs in this region, and therefore it is important for us to obtain insight on the accumulation tendency of this region. As a representative system, we have chosen the 3 tau system, and Fig. 5a shows the snapshots at the beginning, intermediate stage, and end of the simulation for both cases. Fig. 5b shows the comparison of relative distances in three-dimensional space between the tau proteins in normal and phosphorylated states for all cases. Due to the irregular shape of tau protein, the distances between the overall mass centers do not reflect much on the tau accumulation, but the distances between the mass centers of the projection domains of the tau proteins placed in vicinity of each other do. For example, the projection domain mass center distances in the three dimensional space are approximately 15 Å, 20 Å and 18 Å less for phosphorylated tau proteins than the normal tau proteins for protein 1 to protein 2, protein 2 to protein 3 and protein 3 to protein 1 respectively in the 3 tau system, which essentially suggests the tendency of tau accumulation in phosphorylated state. It is to be mentioned that for 2 and 3 tau systems, the projection domain mass center distances are reported by showing distances for all the combinations. However, for 4 tau system, it is only meaningful to report the distance between the projection domains of protein 1 and protein 4, as the system is created by offsetting protein 1 at a 40 Å distance in the z direction, and therefore, protein 1 will tend to interact with the projection domain of the nearest neighbor, which is protein 4. For the same reason, the only insightful way to quantify the decrease of distances at phosphorylated condition is to report the following distances: protein 1 to protein 4, protein 2 to protein 5, and protein 3 to protein 6. Fig. 5b summarizes the observation that in all systems, residue phosphorylated proteins show less distance than the normal ones, which suggests greater accumulation tendency.

4. Discussion

In this study, we have analyzed the response of tau protein and tau-MT interaction from a mechano-chemical point of view to address a current limitation in the literature manifested by absence of comprehensive study on tau protein mechanical behavior (Khan et al., 2020). We have performed tensile tests on a predicted structure of tau protein to determine the single tau projection domain stiffness, dimerized tau separation stretch, tau-MT separation stretch, and compared tau accumulation tendency in non-phosphorylated and phosphorylated states in nanosecond time scale. For a disordered protein, the confidence score (C-score) of −0.03 has been assumed as reliable in our simulation. The detail of quantification of the reliability for a protein structure predicted by i-TASSER (Zhang, 2008) is discussed in the supplementary material of this manuscript. It is to be noted that several reference are repeated in this manuscript due to relevance to the mechano-chemical viewpoint, and are discussed in detail in the discussion section on our earlier work on tau protein, which observed tau and tau-MT phenomena from strictly mechanical perspective.

From our extensive literature review, application of high strain rate and the resulting unfolding and stretching alone do not induce any

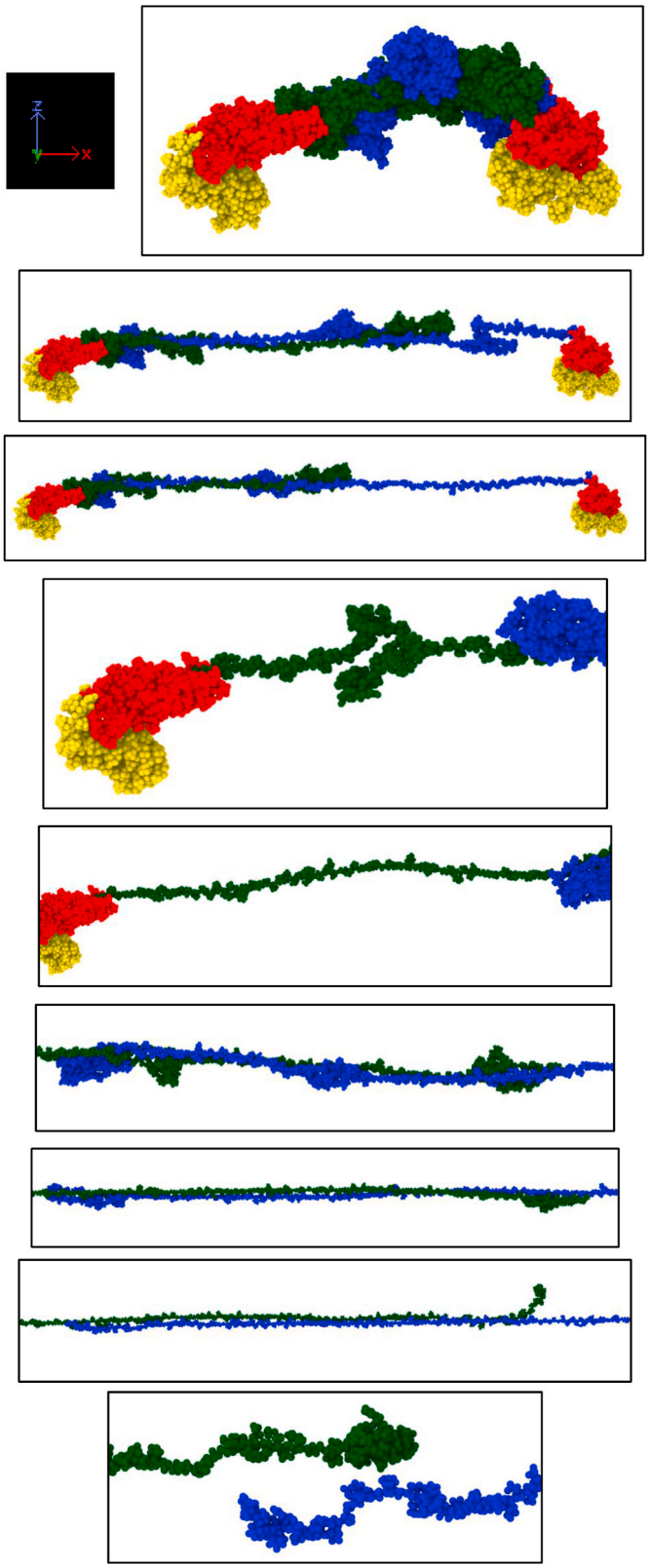

(caption on next column)

Fig. 2b. Stages observed during the pull of one protein in the dimerized tau model (normal phosphorylation, strain rate: $2 \times 10^{9}s^{-1}$). i. Initial stage (strain: 0%), ii. Unfolding of protein 2 (strain: 135%), iii. Stretching of protein 2 (strain: 177%), iv. Unfolding of protein 1 (strain: 325%), v. stretching of protein 1 (strain: 345%), vi. Disentanglement of the overlapped projection domains of the tau proteins (strain: 430%), vii. Continued disentanglement (strain: 676%), viii. Sliding out of projection domain (strain: 750%), ix. Separation of proteins (strain: 758%). Color legends: Green: Projection domain of protein 2, Blue: projection domain of protein 1, Red: MT binding region (including the inter-repeats) for protein 1 and 2, Yellow: N terminal tails of protein 1 and 2. (For interpretation of the references to colour in this figure legend, the reader is referred to the Web version of this article.)

phosphorylation-related symptom or disease in human body, but phosphorylation state significantly manipulates the manner of unfolding, stretching, and tau-MT binding affinity as found by our results. This study is performed to provide a novel insight on simultaneous mechanical loading and phosphorylation effect on tau protein. Existent literature shows that aside from tau protein being a biomarker of TBI, its behavior such as tau-MT affinity, unfolding, etc. strongly depend on the phosphorylation state. Therefore, it is important to discuss the mechanical behavior of tau protein according to domain-phosphorylated and residue-phosphorylated states. In other words, from the TBI perspective, it is important to obtain insight regarding the extent of injury of a person affected by brain injury due to exposure to blast wave and resulting mechanical loading on axonal cytoskeleton components of neuron. Indeed, a more comprehensive insight is obtained if we incorporate the biochemical effect, as the tau-MT affinity is hypothesized to be significantly dependent upon the phosphorylation state. In a nutshell, this study investigates simultaneous mechanical loading (brain trauma) and biochemical phenomena (domain phosphorylation and residue phosphorylation).

For our simulations, we have utilized CHARMM force field. However, there are several other alternative force field, such as COMPASS (McQuaid et al., 2004), or reactive force field like ReaxFF (Senftle et al., 2016). However, in our case, the main objective is to capture large deformation, which requires large simulation box size. For such large systems associated with significant unfolding and stretching, using ReaxFF is highly expensive. Furthermore, recently published work on microtubules has shown that CHARMM can successfully capture the deformation associated with high strain rate (Wu and Adnan, 2018).

The strain rates that we have applied fall into high to very high range. It is possible to deduct the response of our systems under more realistic strain rate by using Bell's theorem (Buehler and Ackbarow, 2007), which suggests that material behaves as more stiffer when applied strain rate is increased due to logarithmic increment of rupture force of intermolecular bond (Ahmadzadeh et al., 2014). Considering these aspects of this theorem, this could be a possible future direction. However, the range of strain rate we have used is relevant to TBI scenario, especially in the length scale of the simulations we have performed. In reality, moderate level blow on the head may lead to high level tissue deformation, which eventually leads to extreme level of stress and failure in sub-axonal level components, supported by recent finite element method (FEM) studies on axon (Cloots et al, 2010, 2011). These studies show that axonal level anisotropy and cellular level heterogeneity might play instrumental role to determine failure criteria of the components, and injury level. Also, this level of strain rate is justified in the scenario of cavitation bubble collapse or blast wave exposure, which leads to intensely high stress in sub-axonal component (Wu and Adnan, 2018).

Phosphorylation effect on tau protein and its ability to alter mechanical behavior has been hypothesized as an important parameter in cytoskeletal studies, but the causal postulates have been dubious for multiple reasons. Experimental studies have already shown that aggregation can be phosphorylation independent (Goedert et al., 1992) and healthy to disordered conformation is reversible (Biernat et al., 1992).

Table 4
Observation of tau-MT interaction for phosphorylation at different domains (strain rate: $2 \times 10^9\ s^{-1}$).

Phosphorylation	MT Binding Site Separation (Strain, %)
Normal	1125
Projection	1330
MT Binding Site	No (Up to 2000%)
Tail	1330
All	918

First, due to the dynamic nature of tau-MT interaction scenario, it is postulated that phosphorylation is not the only parameter and a dynamic combination of several biochemical parameters have ability to alter tau behavior (Churcher, 2006; Lindwall and Cole, 1984), and that multiple parameters might play crucial role to invoke a certain single physical or chemical response (Churcher, 2006). Second, healthy versus phosphorylated tau protein vulnerability to instability under mechanical load has not been quantified. Admittedly, quantification from this outlook is difficult because phosphorylation is not only developmentally regulated (Dudek and Johnson, 1995; Goode and Feinstein, 1994), but also dependent on stoichiometry and number of tubulin dimer attached in phosphorylated state, which may invoke less sensitivity to phosphorylation effect (Gustke et al., 1994). The absence of causal relationships between the mechanism of phosphorylation and its effect was the primary motivation of the current study, and essentially the results provide new insight from both perspectives.

In order to avoid overemphasizing on solely phosphorylation effect, the quantification of both domain focused and residue focused phosphorylation must be considered. From that perspective, the healthy versus considerably phosphorylated tau protein response under extreme mechanical load has been documented in this manuscript, where the phosphorylation level from the literature and in this manuscript are comparable. Moreover, MD simulation has proven to be particularly useful in the current study, as we have been able to observe tau protein behavior in realistic environment in nanometer length scale, retaining the atomistic details.

The general observation is negligible to no sensitivity of domain focused phosphorylation to mechanical load, whereas higher level sensitivity of residue focused phosphorylation suggests the importance of targeting specific residues in critical region around MT binding region, and justifies the tendency of kinases of attacking active sites in the side chains of tau protein filament and interrepeat regions of MT binding sites. From the literature it is already evident that not all phosphorylation sites play equally significant role to determine tau-MT interaction, and therefore, a more comprehensive residue-by-residue phosphorylation effect study would provide more complete insight on the effect of strain rate in presence of posttranslational modification at different domains or residues. However, after comprehensive literature review on this aspects, the author would recommend practicing reservation while selecting phosphorylation sites, as single site phosphorylation can affect the tau-MT affinity, but not strong enough to overlook other effects; and due to possible clustering effects, mutually exclusive combination of

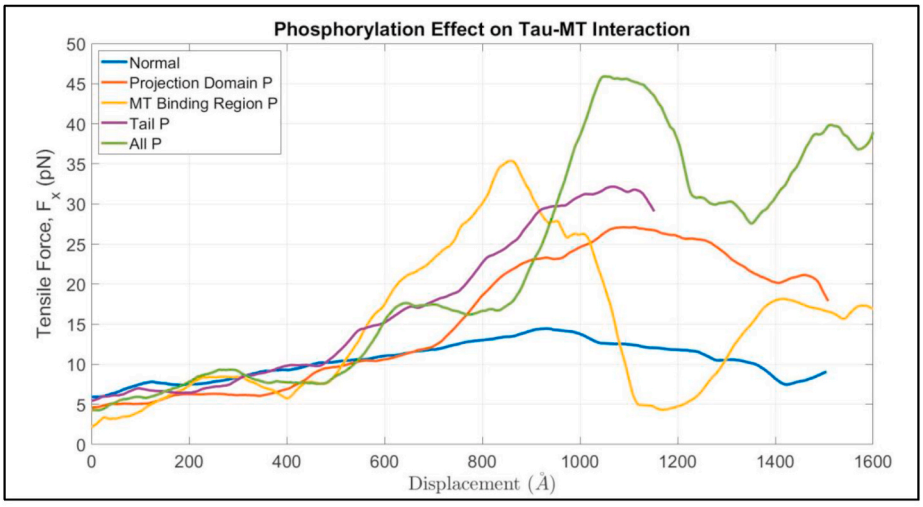

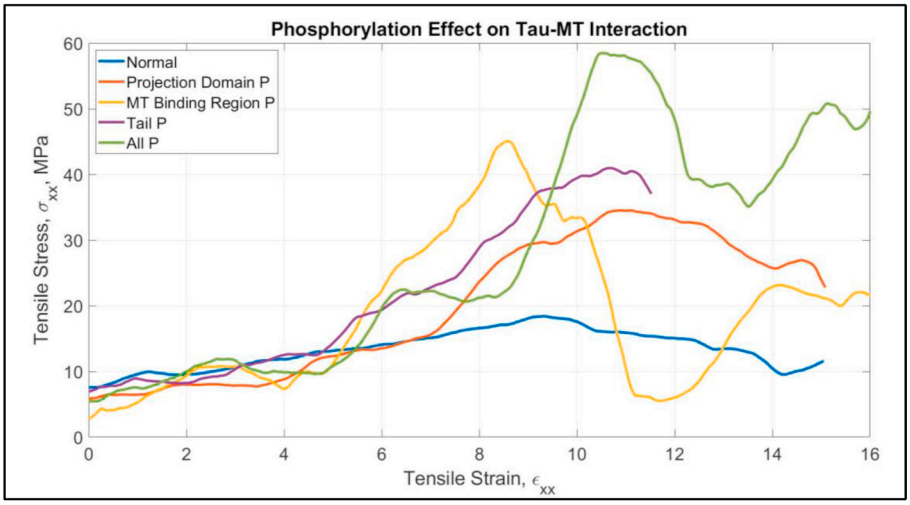

Fig. 3a. Figure 3a i. Force-displacement and ii. Stress-vs Strain graph for the projection domain of tau during the pulling from MT (strain rate: $2 \times 10^9 s^{-1}$). For normal phosphorylation, separation occurs at ~1125% strain. For phosphorylation in projection domain and N-terminus tail, it occurs at ~1330% strain. For phosphorylation in MT binding sites, it does not occur (we have continued the simulation for this case up to 2000%). For phosphorylation in all domains, the separation occurs at ~918%. Data smoothened by using moving average.

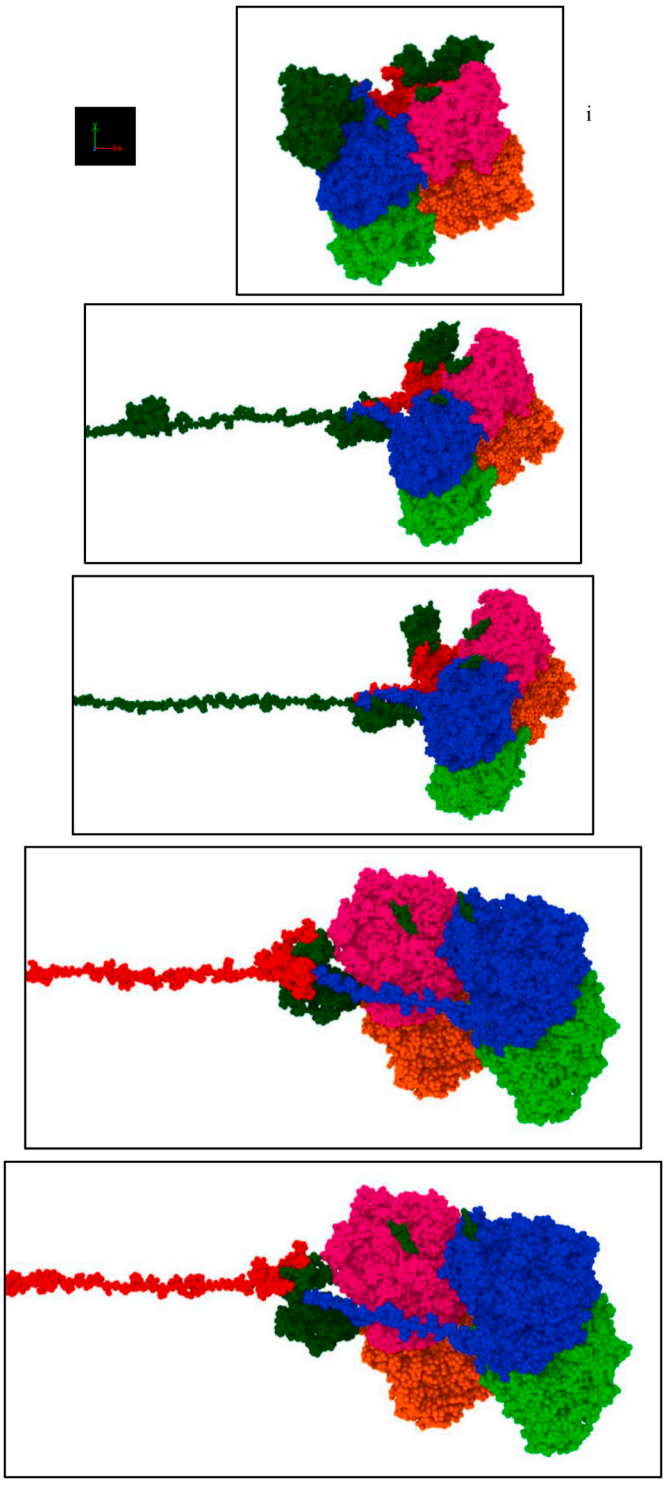

Fig. 3b. Observation during the pulling of tau along -x direction (normal phosphorylation, strain rate: $2 \times 10^{9} s^{-1}$). i. Initial stage (strain: 0%), ii. Unfolding of tau projection domain (strain: 376%), iii. Stretching of tau projection domain (strain: 640%), iv. Onset of tau MT binding region separation (strain: 1095%), v. Separation of MT binding region from MT surface (strain: 1125%). Color legends: dark green: tau, red: MT binding region of tau (including the interrepeats), orange: α subnit 1, pink: β subnit 1, blue: α subnit 2, light green: β subnit 2, white: GDP and GTP atoms and Mg^{2+} ion. (For interpretation of the references to colour in this figure legend, the reader is referred to the Web version of this article.)

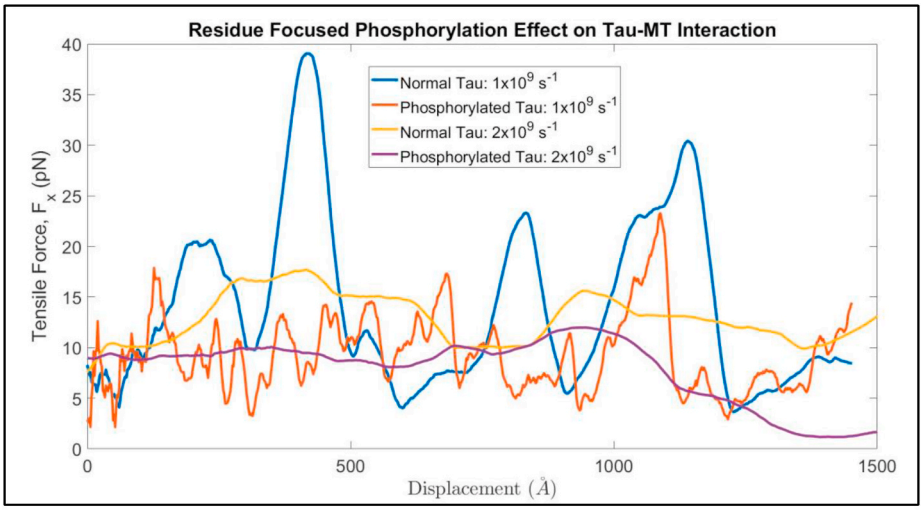

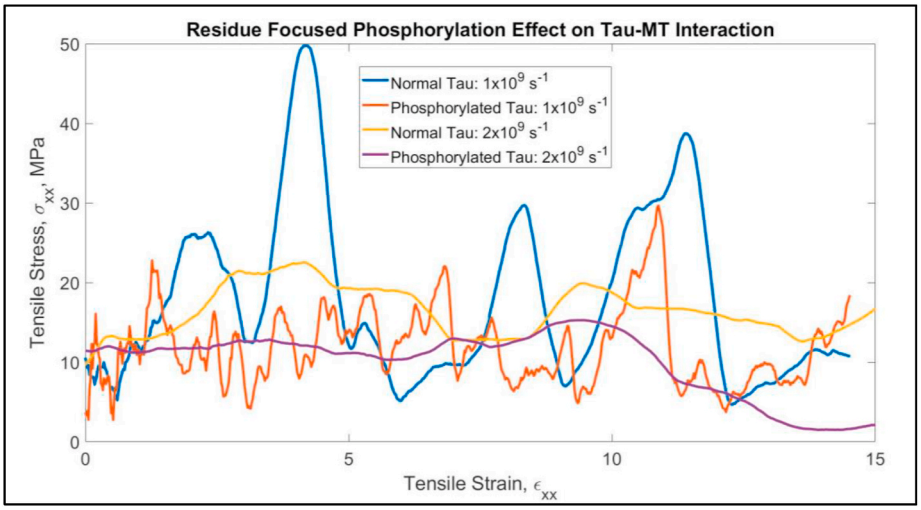

Fig. 4a. Figure 4a i. Force vs Displacement and ii. Stress vs Strain graph for the projection domain of tau during the pulling from MT. At the strain rate of $10^9 s^{-1}$, for normal phosphorylation, separation occurs at ~1193% strain, while for phosphorylated tau, it occurs at ~1100% strain. At the strain rate of $2 \times 10^9 s^{-1}$, for normal phosphorylation, separation occurs at ~1170% strain, while for phosphorylated tau, it occurs at ~1060% strain. The continuous unfolding and stretching patterns are similar for both cases. Data smoothened by using moving average.

phosphorylation sites might be equally strong candidates to alter the mechanical behavior of tau and tau-MT interaction.

Earlier studies have repetitively suggested that residue-focused studies can provide more quantitative insight than the domain-focused ones, and that a representative pathological state of tau would consist of 7–8 phosphorylated sites (Jho et al., 2010; Kenessey and Yen, 1993). Furthermore, from the domain point of view, the projection domain in the vicinity of MT binding region, and the interrepeat domains in the MT binding region are the strongest candidates to alter tau-MT binding affinity. Therefore, the current study can reliably represent the phosphorylation effect from both phosphorylation level and active site location standpoints; and especially the observation from the residue-focused tau-MT interaction results further substantiates the selection of active phosphorylation sites in this region. Our selection of critical phosphorylation sites SER 199, 202, 262, 396, 404, 409, and THR 231) takes the possibility of weakening the cytoskeleton into account, as well as attempts to highlight the effect of phosphorylation effect outside MT binding region, which were not conclusive in the earlier studies (Biernat et al., 1992; Bramblett et al., 1993; Buerger et al., 2002; Haense et al., 2008; Hu et al., 2002; Kenessey and Yen, 1993; Mandelkow and Mandelkow, 1998; Mandelkow et al., 1995; Pickhardt et al., 2005; Santarella et al., 2004; Trinczek et al., 1995).

The response of single tau, dimerized tau, and tau-MT interaction in presence of domain-focused phosphorylation suggested that phosphorylation effect in different domains or multiple domains simultaneously might be ineffective in presence of extreme mechanical load. On the other hand, residue-focused phosphorylation in tau-MT system and tau accumulation system suggested strong effect of phosphorylation irrespective of mechanical loading, substantiating the relative importance of residues from the perspective of phosphorylation.

Admittedly, the accumulation tendency is likely to be a function of primary conformation also, and therefore, a continuation of this study might consist of a statistical significance of primary conformation of tau protein, and concentration in a given system size to obtain quantitative insight on the aggregation tendency. In order to verify the dependence of multiple tau protein accumulation on the residue phosphorylation state, we have tested four (4) systems with 2, 3, 4, and 6 tau proteins. In all cases, we have observed that phosphorylated tau proteins tend to accumulate more than the normal ones. It is relevant to mention that between microtubule (MT) bundles, tau protein acts as crosslinks, and they are spaced 20–40 nm from each other (Ahmadzadeh et al., 2014; Adnan et al., 2018; Hirokawa et al., 1988; Tang-Schomer et al., 2009). Therefore, for the tensile tests, there is no sample size effect, as one tau protein crosslink does not affect the behavior of another one.

As an intrinsically disordered protein (IDP), the unique responses of tau protein can likely be attributed to its inherent disorder and ever-changing conformation, which might facilitate absorbing strain and extended attachment to MT surface despite extreme strain rate. We consider the scenarios presented as particularly relevant to TBI scenario, as sub-axonal components undergo extreme deformation, and therefore, vulnerable regions would be projection domain of single tau, overlapped projection domains of dimerized tau, and tau-MT interface – as the

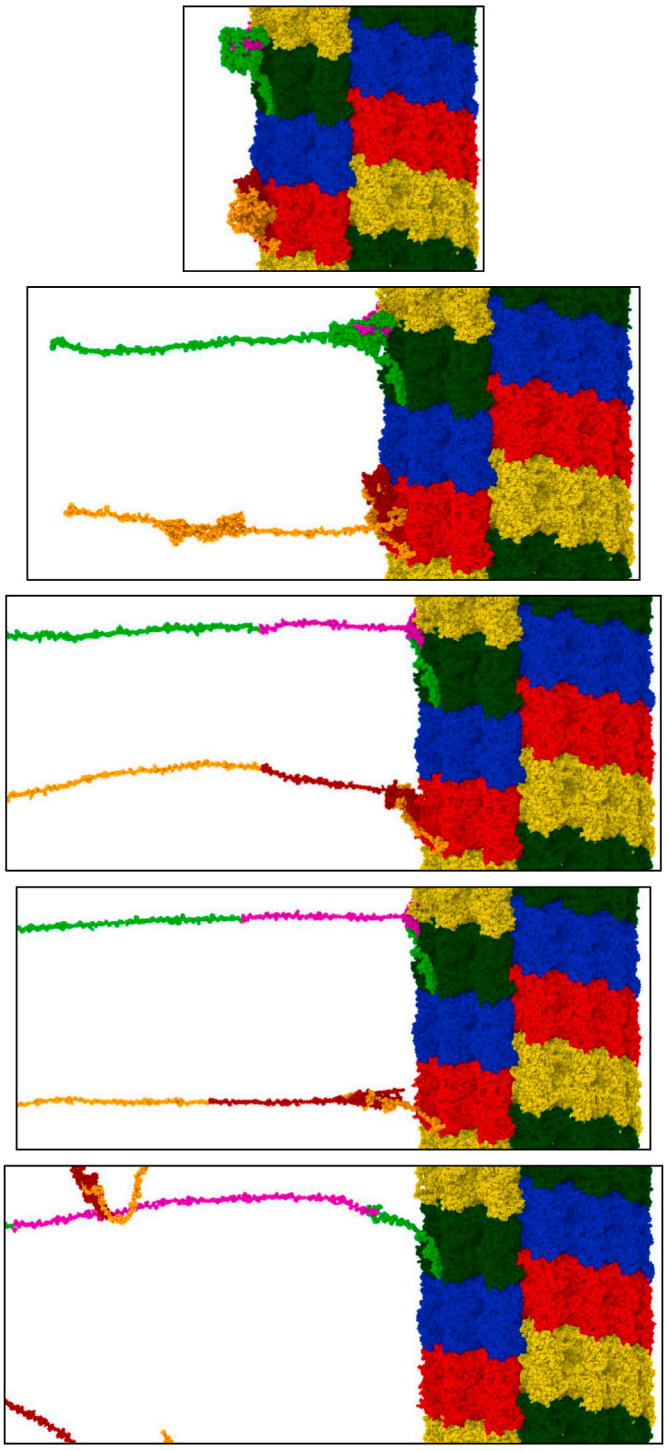

Fig. 4b. Observation during the pulling of tau in the x direction (normal phosphorylation, strain rate: $2 \times 10^{9}s^{-1}$). i. Initial stage (strain: 0%), ii. Unfolding of tau projection domain (strain: 228%), iii. Stretching of tau projection domain (strain: 932%), iv. MT binding region separation for the phosphorylated tau (strain: 1060%), v. MT binding region separation for normal tau (strain: 1170%). Color legends: Red, blue, green and yellow: repeating helical units of MT, light green: projection domain and tail of normal tau, pink: MT binding region of normal tau (including the interrepeats), orange: projection domain and tail of phosphorylated tau, maroon: MT binding region of phosphorylated tau (including the interrepeats). (For interpretation of the references to colour in this figure legend, the reader is referred to the Web version of this article.)

primary markers in TBI are axonal strain and stretch, and deformation of individual components. Furthermore, the accumulation study is also relevant from TBI perspective, as TBI and similar neurological disorders suggest increased tau aggregation. However, as we have mentioned in our mechanical study on tau, a possible continuation is a quantitative assessment of IDP-substrate bonding in presence of mechanical loading and posttranslational modification to decide whether this enhanced interaction is a common attribute of IDPs, especially microtubule-associated proteins. Additionally, the current study also substantiates the importance of studying prolin-rich proteins, which are relevant to neurodegenerative diseases. studies (Gladkevich et al., 2007; Sochocka et al., 2019). These proteins are heavily implicated in neurodegenerative diseases and traumatic brain injury, which tau is also involved in. The prolin-rich region (PRR) is a speculative binding site in proteins, so future studies could highlight on protein-protein interactions from biochemical outlook.

Finally, the multiscale modeling aspect of our study can also be a highly potent future direction. In the earlier section of the discussion, we have already substantiated that the extent of injury differs from length scale to length scale, and that mild injury to the head at macroscale may cause significant deformation in tissue level, leading to eventual extreme deformation at axonal level (Cloots et al., 2010). Therefore, the strain-rate dependent behavior of the tau protein (and other axonal cytoskeletal components of neuron) can be used to develop a bottom-up realistic and comprehensive axon model. In this regard, one approach could be determining damage-prone areas of brain by using continuum scale model of highly biofidelic human head (Pearce and Young, 2014), and then incorporate the cellular and axonal level properties to validate the behavior of the model. It is to be noted that multiscale modeling by using combination of MD simulation and finite element method (FEM) has been used in diversified fields of materials science, such as Li-ion battery development, (Mortazavi et al., 2017), graphene composite structure (Mortazavi and Rabczuk, 2015), etc.

5. Conclusion

In this paper, we have attempted to determine the unfolding and stretching stiffness for single tau, stretching required for dimerized tau and tau-MT interaction models, and find the effect of phosphorylation on different domains of tau on these particular mechanical properties or behaviors. From our simulations, the major findings can be summarized as below:

1. Single tau protein does not show dynamic alteration in unfolding and stretching stiffness due to phosphorylation and stretching stiffness can be 4–7 times higher than the unfolding stiffness.
2. Dimerized tau protein models show that the stretching required to separate the protein forming the dimer is the same for phosphorylation in individual domains (~750%), but is significantly less in case of phosphorylation in all domains (~600%).
3. For tau-MT interaction simulations, it is found that for normal phosphorylation, the tau separation from MT occurs at ~1125% strain, but for phosphorylation in projection domain and N-terminus tail, it occurs at higher strain (~1330%), for phosphorylation in MT binding sites, MT-tau shows the strongest bond that cannot be separated even at the cost of disintegration of MT subunits, and separation takes place earlier for phosphorylation in all domains altogether (~918%).
4. Phosphorylated tau separates earlier from the MT surface than normal tau. However, the separation stretch is different according to the strain rate. At higher strain rate, the normal tau separates at 1170% strain, while phosphorylated one separates at 1060% strain. At lower strain rate, the normal tau and phosphorylated tau separate at 1193% and 1100% strain, respectively.
5. Normal tau and phosphorylated tau show different accumulation tendency. For 1ns NVT equilibration at 310 K, randomly placed tau

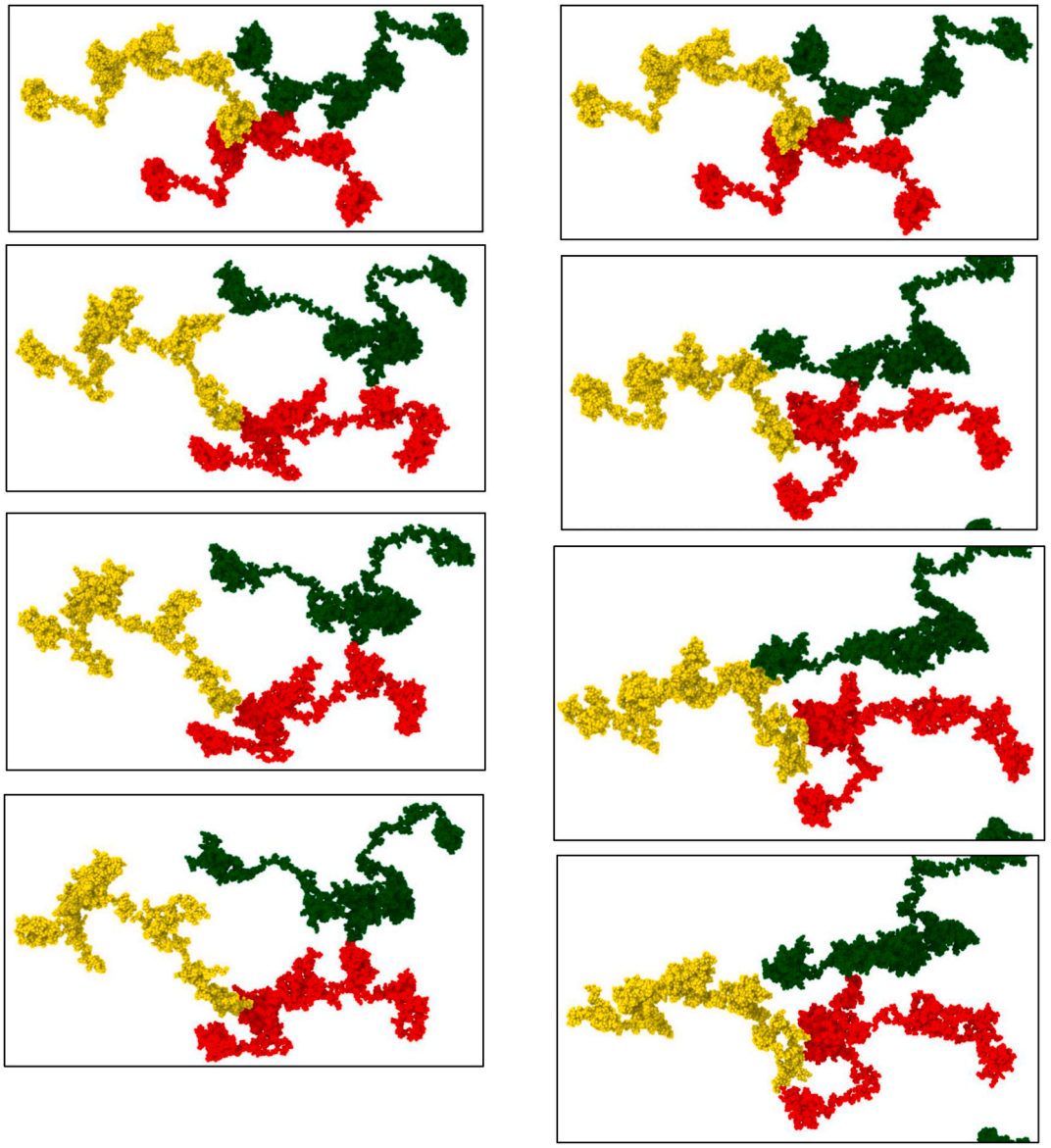

Fig. 5a. Snapshots at different times during the 1ns NVT equilibration for normal and phosphorylated taus (at 7 sites). For phosphorylated taus, tendency to decrease the distance between the proteins is observed. i. Normal tau: 0 ps, ii. Normal tau: 100 ps, iii. Normal tau: 500 ps, iv. Normal tau: 1 ns, v. Phosphorylated tau: 0 ps, vi. Phosphorylated tau: 100 ps, vii. Phosphorylated tau: 500 ps, viii. Phosphorylated tau: 1 ns? Color legends: Red: protein 1, Green: protein 2, Yellow: protein 3. (For interpretation of the references to colour in this figure legend, the reader is referred to the Web version of this article.)

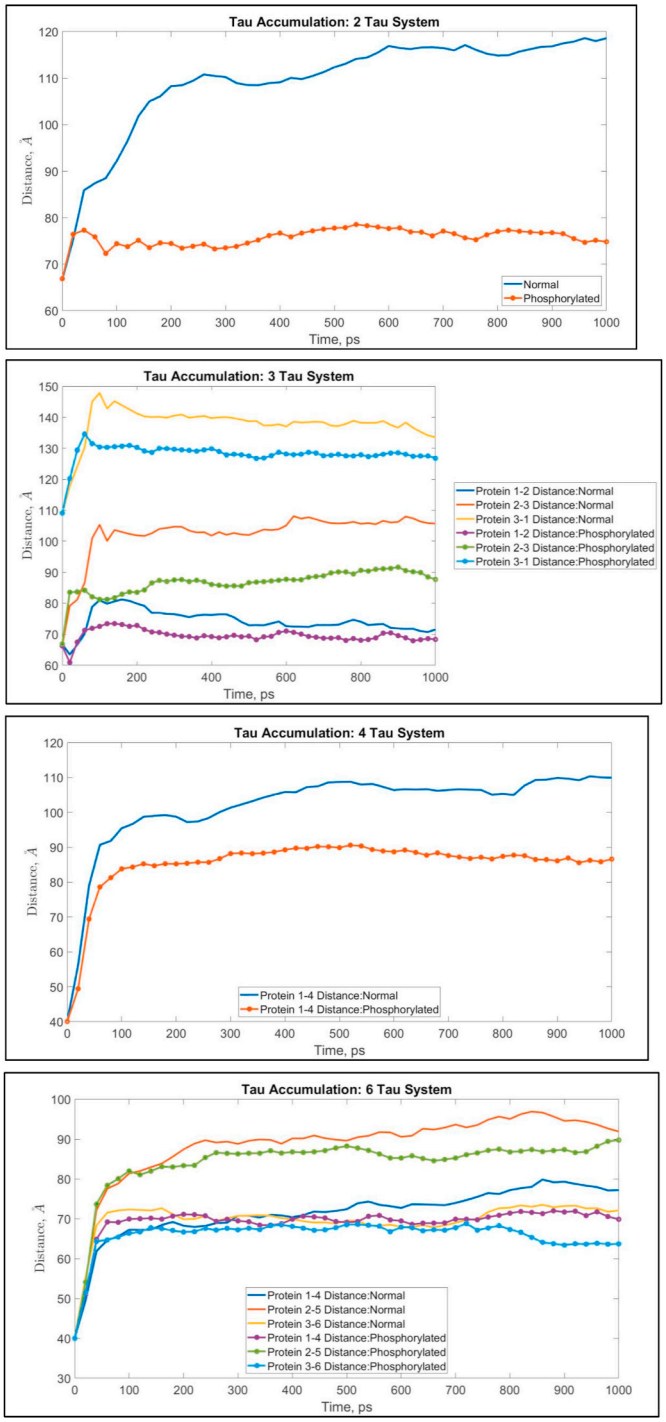

Fig. 5b. Projection domain mass center distance of the proteins as a function of time. i. 2 tau system, ii. 3 tau system, iii. 4 tau system, iv. 6 tau system.

proteins maintain their distance from each other, while the distance decreases significantly for phosphorylated taus.

Although bottom-up modeling of axon requires mechanical characterization of individual neural cytoskeletal components, the physical chemistry perspective is essential due to their relevance in real-life scenario. Therefore, this study has shown the outcome of some unique approaches to depict mechano-chemical behavior of tau protein, where we can observe the effect of both posttranslational modification, and mechanical response under extreme strain rate, which is relevant to TBI; and this particularly facilitates obtaining insight on comparison between the behavior of healthy and pathological tau.

Declaration of competing interest

The authors declare that they have no known competing financial interests or personal relationships that could have appeared to influence the work reported in this paper.

Acknowledgements

This work has been funded by the Computational Cellular Biology of Blast (C2B2) program through the Office of Naval Research (ONR) (Award #N00014-18-1-2082- Dr. Timothy Bentley, Program Manager). The authors acknowledge the Texas Advanced Computing Center (TACC) at The University of Texas at Austin for providing HPC resources that have contributed to the research results reported within this paper. URL: http://www.tacc.utexas.edu.

Appendix 1. Potential Energy vs Time Graphs

We have plotted potential energy vs time for the dimerized tau, tau-MT, and tau accumulation test for both normal and phosphorylated systems. For dimerized tau and tau-MT systems, these curves are plotted to determine whether any energetical artifacts generate due to the separation of tau from tau or tau from MT surface. In the accumulation test, we plot potential energy vs time to ensure that both systems are well equilibrated. In this appendix, the potential energy vs time graphs are presented.

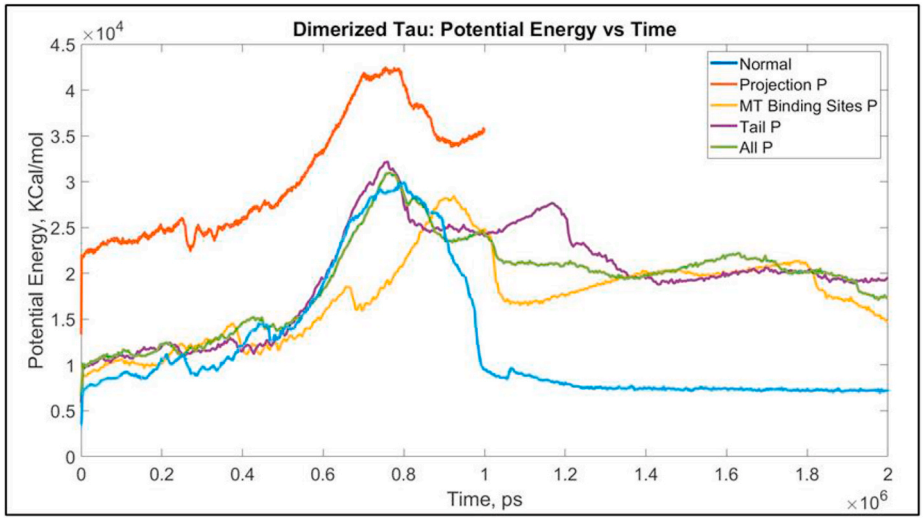

Fig. A1. Dimerized tau: potential energy vs time for the domain phosphorylated systems.

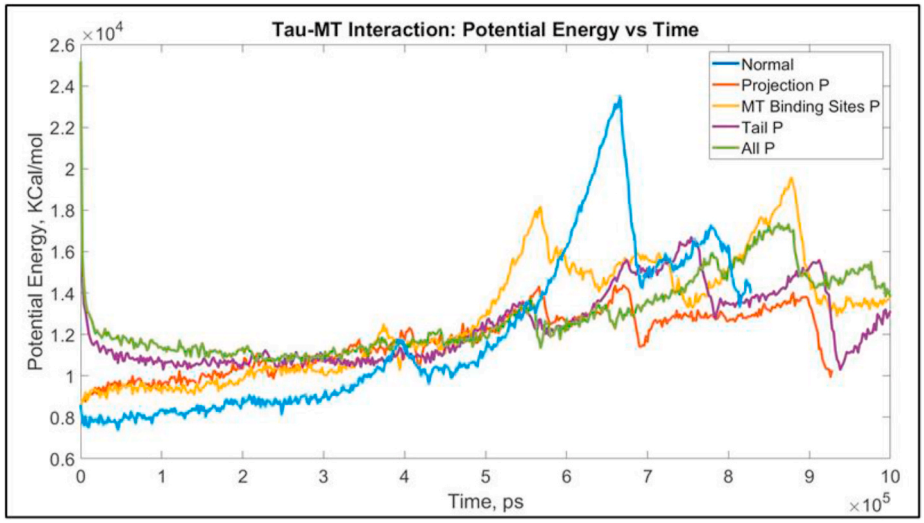

Fig. A2. Tau-MT interaction: potential energy vs time for the domain phosphorylated systems. .

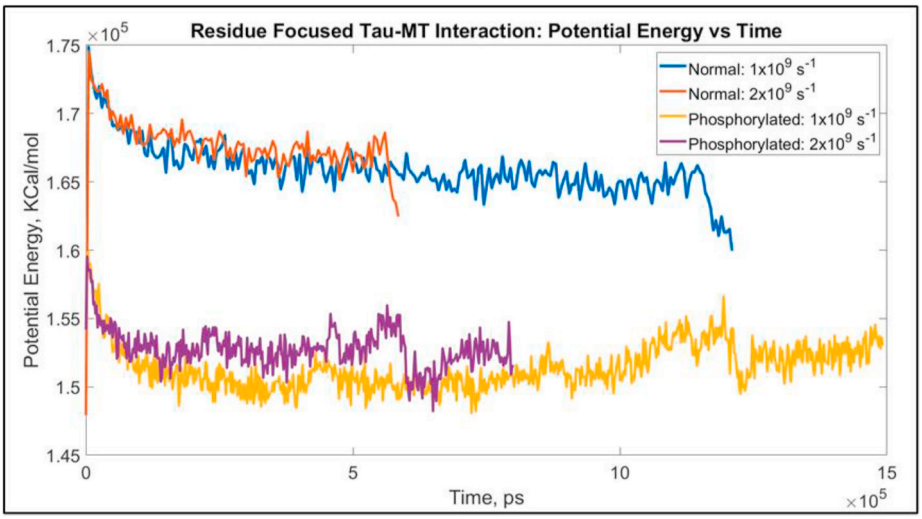

Fig. A3. Tau-MT interaction: potential energy vs time for the residue phosphorylated systems. .

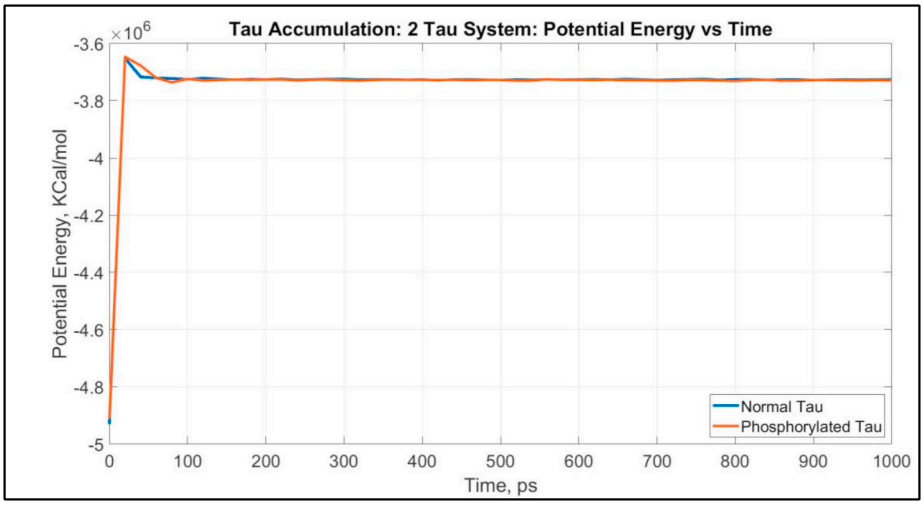

Fig. A4. Tau accumulation test: 2 tau system: potential energy vs time during the 1ns equilibration. .

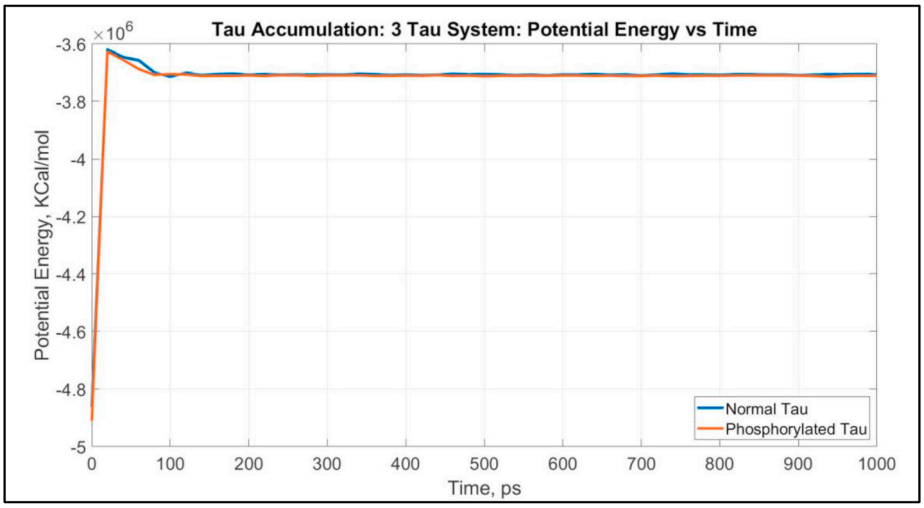

Fig. A5. Tau accumulation test: 3 tau system: potential energy vs time during the 1ns equilibration.

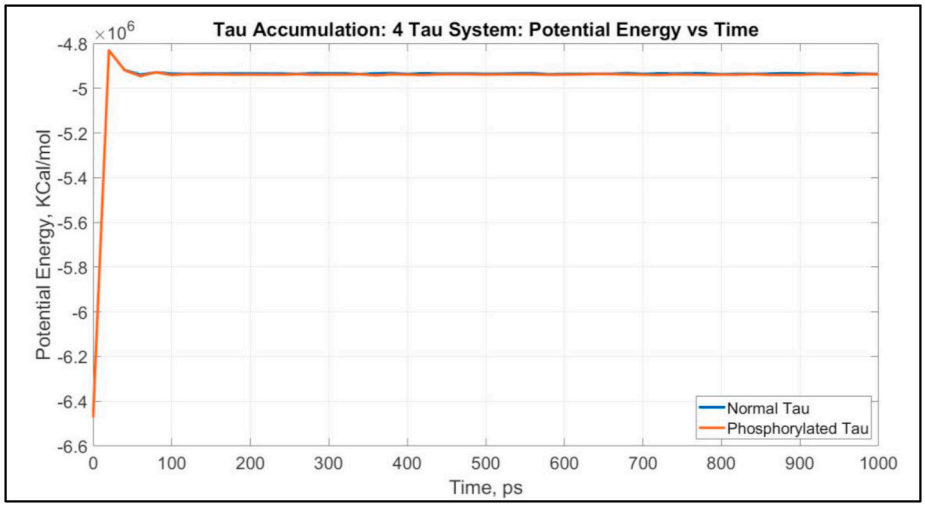

Fig. A6. Tau accumulation test: 4 tau system: potential energy vs time during the 1ns NVT equilibration. .

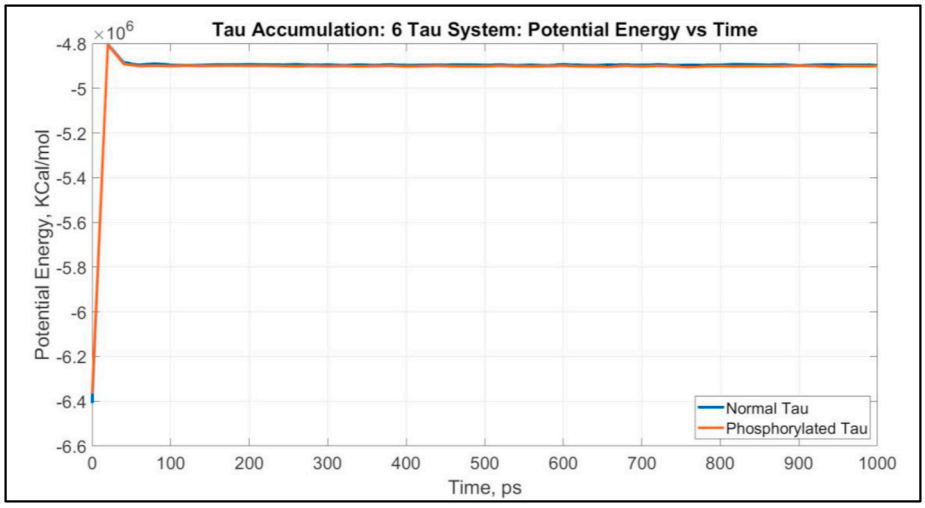

Fig. A7. Tau accumulation test: 6 tau system: potential energy vs time during the 1ns NVT equilibration.

Author contributions

M.I.KA.AFH, KAM, .

References

Adnan, Ashfaq, Siddiq, Qidwai, Amit, Bagchi, 2018. On the atomistic-based continuum viscoelastic constitutive relations for axonal microtubules. J. Mech. Behav. Biomed. Mater. 86, 375–389. https://doi.org/10.1016/j.jmbbm.2018.06.031.

Ahmadzadeh, H., Smith, D.H., Shenoy, V.B., 2014. Viscoelasticity of tau proteins leads to strain rate-dependent breaking of microtubules during axonal stretch injury: predictions from a mathematical model. Biophys. J. 106, 1123–1133. https://doi.org/10.1016/j.bpj.2014.01.024.

Alonso, A. del C., Mederlyova, A., Novak, M., Grundke-Iqbal, I., Iqbal, K., 2004. Promotion of hyperphosphorylation by frontotemporal dementia tau mutations. J. Biol. Chem. 279, 34873–34881.

Avila, J., 1990. Microtubule dynamics. Faseb. J. 4, 3284–3290. https://doi.org/10.1096/fasebj.4.15.2253844.

Ballatore, C., Lee, V.M.-Y., Trojanowski, J.Q., 2007. Tau-mediated neurodegeneration in Alzheimer's disease and related disorders. Nat. Rev. Neurosci. 8, 663.

Battisti, A., Ciasca, G., Grottesi, A., Bianconi, A., Tenenbaum, A., 2012. Temporary secondary structures in tau, an intrinsically disordered protein. Mol. Simulat. 38, 525–533.

Baudier, J., Cole, R.D., 1987. Phosphorylation of tau proteins to a state like that in Alzheimer's brain is catalyzed by a calcium/calmodulin-dependent kinase and modulated by phospholipids. J. Biol. Chem. 262, 17577–17583.

Becker, J.S., Przybylski, M., 2007. Studies of structure and phosphorylation of tau protein using high resolution mass spectrometry. J. Anal. At. Spectrom. 22, 761–765.

Best, R.B., Zhu, X., Shim, J., Lopes, P.E.M., Mittal, J., Feig, M., MacKerell, A.D., 2012. Optimization of the additive CHARMM all-atom protein force field targeting improved sampling of the backbone φ, ψ and side-chain χ1 and χ2 dihedral angles. J. Chem. Theor. Comput. 8, 3257–3273. https://doi.org/10.1021/ct300400x.

Biernat, J., Gustke, N., Drewes, G., Mandelkow, E., 1993. Phosphorylation of Ser262 strongly reduces binding of tau to microtubules: distinction between PHF-like immunoreactivity and microtubule binding. Neuron 11, 153–163.

Biernat, J., Mandelkow, E.M., Schröter, C., Lichtenberg-Kraag, B., Steiner, B., Berling, B., Meyer, H., Mercken, M., Vandermeeren, A., Goedert, M., 1992. The switch of tau protein to an Alzheimer-like state includes the phosphorylation of two serine-proline motifs upstream of the microtubule binding region. EMBO J. 11, 1593–1597.

Billingsley, M.L., Kincaid, R.L., 1997. Regulated phosphorylation and dephosphorylation of tau protein: effects on microtubule interaction, intracellular trafficking and neurodegeneration. Biochem. J. 323, 577–591.

Bramblett, G.T., Goedert, M., Jakes, R., Merrick, S.E., Trojanowski, J.Q., Lee, V.M.Y., 1993. Abnormal tau phosphorylation at Ser396 in Alzheimer's disease recapitulates development and contributes to reduced microtubule binding. Neuron 10, 1089–1099.

Brandt, R., Lee, G., 1993. Functional organization of microtubule-associated protein tau. Identification of regions which affect microtubule growth, nucleation, and bundle formation in vitro. J. Biol. Chem. 268, 3414–3419.

Brooks, B.R., Brooks III, C.L., Mackerell Jr., A.D., Nilsson, L., Petrella, R.J., Roux, B., Won, Y., Archontis, G., Bartels, C., Boresch, S., Caflisch, A., Caves, L., Cui, Q., Dinner, A.R., Feig, M., Fischer, S., Gao, J., Hodoscek, M., Im, W., Kuczera, K., Lazaridis, T., Ma, J., Ovchinnikov, V., Paci, E., Pastor, R.W., Post, C.B., Pu, J.Z., Schaefer, M., Tidor, B., Venable, R.M., Woodcock, H.L., Wu, X., Yang, W., York, D. M., Karplus, M., 2009. CHARMM: the biomolecular simulation program. J. Comput. Chem. 30, 1545–1614. https://doi.org/10.1002/jcc.21287.

Buck, M., Bouguet-Bonnet, S., Pastor, R.W., MacKerell, A.D., 2006. Importance of the CMAP correction to the CHARMM22 protein force field: dynamics of hen lysozyme. Biophys. J. 90, L36–L38. https://doi.org/10.1529/biophysj.105.078154.

Buée, L., Bussière, T., Buée-Scherrer, V., Delacourte, A., Hof, P.R., 2000. Tau protein isoforms, phosphorylation and role in neurodegenerative disorders. Brain Res. Rev. 33, 95–130.

Buehler, M.J., Ackbarow, T., 2007. Fracture mechanics of protein materials. Mater. Today 10, 46–58.

Buerger, K., Zinkowski, R., Teipel, S.J., Tapiola, T., Arai, H., Blennow, K., Andreasen, N., Hofmann-Kiefer, K., DeBernardis, J., Kerkman, D., 2002. Differential diagnosis of Alzheimer disease with cerebrospinal fluid levels of tau protein phosphorylated at threonine 231. Arch. Neurol. 59, 1267–1272.

Castro, T.G., Munteanu, F.-D., Cavaco-Paulo, A., 2019. Electrostatics of tau protein by molecular dynamics. Biomolecules 9, 116.

Chau, M.-F., Radeke, M.J., de Inés, C., Barasoain, I., Kohlstaedt, L.A., Feinstein, S.C., 1998. The microtubule-associated protein tau cross-links to two distinct sites on each α and β tubulin monomer via separate domains. Biochemistry 37, 17692–17703.

Churcher, I., 2006. Tau therapeutic strategies for the treatment of Alzheimer's disease. Curr. Top. Med. Chem. 6, 579–595.

Cleveland, D.W., Hwo, S.-Y., Kirschner, M.W., 1977. Physical and chemical properties of purified tau factor and the role of tau in microtubule assembly. J. Mol. Biol. 116, 227–247.

Cloots, R.J.H., Van Dommelen, J.A.W., Kleiven, S., Geers, M.G.D., 2010. Traumatic brain injury at multiple length scales: relating diffuse axonal injury to discrete axonal impairment. In: Proceedings of IRCOBI Conference, pp. 119–130.

Cloots, R.J.H., Van Dommelen, J.A.W., Nyberg, T., Kleiven, S., Geers, M.G.D., 2011. Micromechanics of diffuse axonal injury: influence of axonal orientation and anisotropy. Biomech. Model. Mechanobiol. 10, 413–422.

Dudek, S.M., Johnson, G.V.W., 1995. Postnatal changes in serine/threonine protein phosphatases and their association with the microtubules. Dev. Brain Res. 90, 54–61.

Ferrer, I., Gomez-Isla, T., Puig, B., Freixes, M., Ribe, E., Dalfo, E., Avila, J., 2005. Current advances on different kinases involved in tau phosphorylation, and implications in Alzheimer's disease and tauopathies. Curr. Alzheimer Res. 2, 3–18.

Fitzpatrick, A.W.P., Falcon, B., He, S., Murzin, A.G., Murshudov, G., Garringer, H.J., Crowther, R.A., Ghetti, B., Goedert, M., Scheres, S.H.W., 2017. Cryo-EM structures of tau filaments from Alzheimer's disease. Nature 547, 185.

Garver, T.D., Lehman, R.A.W., Billingsley, M.L., 1996. Microtubule assembly competence analysis of freshly-biopsied human tau, dephosphorylated tau, and Alzheimer tau. J. Neurosci. Res. 44, 12–20. https://doi.org/10.1002/(SICI)1097-4547(19960401)44:1<12::AID-JNR2>3.0.CO;2-L.

Gladkevich, A., Bosker, F., Korf, J., Yenkoyan, K., Vahradyan, H., Aghajanov, M., 2007. Proline-rich polypeptides in Alzheimer's disease and neurodegenerative disorders—therapeutic potential or a mirage? Prog. Neuro-Psychopharmacol. Biol. Psychiatry 31, 1347–1355.

Goedert, M., Jakes, R., Crowther, R.A., Six, J., Lübke, U., Vandermeeren, M., Cras, P., Trojanowski, J.Q., Lee, V.M., 1993. The abnormal phosphorylation of tau protein at Ser-202 in Alzheimer disease recapitulates phosphorylation during development. Proc. Natl. Acad. Sci. U. S. A. 90, 5066–5070.

Goedert, M., Jakes, R., Spillantini, M.G., Hasegawa, M., Smith, M.J., Crowther, R.A., 1996. Assembly of microtubule-associated protein tau into Alzheimer-like filaments induced by sulphated glycosaminoglycans. Nature 383, 550–553.

Goedert, M., Spillantini, M.G., Cairns, N.J., Crowther, R.A., 1992. Tau proteins of Alzheimer paired helical filaments: abnormal phosphorylation of all six brain isoforms. Neuron 8, 159–168.

Goedert, M., Spillantini, M.G., Jakes, R., Rutherford, D., Crowther, R.A., 1989. Multiple isoforms of human microtubule-associated protein tau: sequences and localization in neurofibrillary tangles of Alzheimer's disease. Neuron 3, 519–526.

Goode, B.L., Feinstein, S.C., 1994. Identification of a novel microtubule binding and assembly domain in the developmentally regulated inter-repeat region of tau. J. Cell Biol. 124, 769–782. https://doi.org/10.1083/jcb.124.5.769. LP.

Götz, J., Probst, A., Spillantini, M.G., Schäfer, T., Jakes, R., Bürki, K., Goedert, M., 1995. Somatodendritic localization and hyperphosphorylation of tau protein in transgenic mice expressing the longest human brain tau isoform. EMBO J. 14, 1304–1313.

Grundke-Iqbal, I., Iqbal, K., Tung, Y.-C., Quinlan, M., Wisniewski, H.M., Binder, L.I., 1986. Abnormal phosphorylation of the microtubule-associated protein tau (tau) in Alzheimer cytoskeletal pathology. Proc. Natl. Acad. Sci. U. S. A. 83, 4913–4917.

Gustke, N., Trinczek, B., Biernat, J., Mandelkow, E.-M., Mandelkow, E., 1994. Domains of tau protein and interactions with microtubules. Biochemistry 33, 9511–9522.

Haense, C., Buerger, K., Kalbe, E., Drzezga, A., Teipel, S.J., Markiewicz, P., Herholz, K., Heiss, W.-D., Hampel, H., 2008. CSF total and phosphorylated tau protein, regional glucose metabolism and dementia severity in Alzheimer's disease. Eur. J. Neurol. 15, 1155–1162.

Hanger, D.P., Anderton, B.H., Noble, W., 2009. Tau phosphorylation: the therapeutic challenge for neurodegenerative disease. Trends Mol. Med. 15, 112–119.

Hawkins, B.E., Krishnamurthy, S., Castillo-Carranza, D.L., Sengupta, U., Prough, D.S., Jackson, G.R., DeWitt, D.S., Kayed, R., 2013. Rapid accumulation of endogenous tau oligomers in a rat model of traumatic brain injury possible link between traumatic brain injury and sporadic tauopathies. J. Biol. Chem. 288, 17042–17050.

Hirokawa, N, Shiomura, Y., Okabe, S., 1988. Tau proteins: the molecular structure and mode of binding on microtubules. J. Cell Biol. 107, 1449–1459.

Hu, Y.Y., He, S.S., Wang, X., Duan, Q.H., Grundke-Iqbal, I., Iqbal, K., Wang, J., 2002. Levels of nonphosphorylated and phosphorylated tau in cerebrospinal fluid of Alzheimer's disease patients: an ultrasensitive bienzyme-substrate-recycle enzyme-linked immunosorbent assay. Am. J. Pathol. 160, 1269–1278.

Iqbal, K., Grundke-Iqbal, I., Smith, A.J., George, L., Tung, Y.-C., Zaidi, T., 1989. Identification and localization of a tau peptide to paired helical filaments of Alzheimer disease. Proc. Natl. Acad. Sci. U. S. A. 86, 5646–5650.

Jho, Y.S., Zhulina, E.B., Kim, M.-W., Pincus, P.A., 2010. Monte Carlo simulations of tau proteins: effect of phosphorylation. Biophys. J. 99, 2387–2397.

Jo, S., Kim, T., Iyer, V.G., Im, W., 2008. CHARMM-GUI: a web-based graphical user interface for CHARMM. J. Comput. Chem. 29, 1859–1865. https://doi.org/10.1002/jcc.20945.

Jorda, J., Xue, B., Uversky, V.N., Kajava, A.V., 2010. Protein tandem repeats–the more perfect, the less structured. FEBS J. 277, 2673–2682.

Kandimalla, R.J.L., Prabhakar, S., Wani, W.Y., Kaushal, A., Gupta, N., Sharma, D.R., Grover, V.K., Bhardwaj, N., Jain, K., Gill, K.D., 2013. CSF p-Tau levels in the prediction of Alzheimer's disease. Biol. Open 2, 1119–1124.

Kenessey, A., Yen, S.-H.C., 1993. The extent of phosphorylation of fetal tau is comparable to that of PHF-tau from Alzheimer paired helical filaments. Brain Res. 629, 40–46.

Khan, M.I., Hasan, F., Al Mahmud, K.A.H., Adnan, A., 2020. Recent computational approaches on mechanical behavior of axonal cytoskeletal components of neuron: a brief review. Multiscale Sci. Eng. 1–15.

Khatoon, S., Grundke-Iqbal, I., Iqbal, K., 1994. Levels of normal and abnormally phosphorylated tau in different cellular and regional compartments of Alzheimer disease and control brains. FEBS Lett. 351, 80–84.

Köpke, E., Tung, Y.-C., Shaikh, S., Alonso, A. del C., Iqbal, K., Grundke-Iqbal, I., 1993. Microtubule-associated protein tau. Abnormal phosphorylation of a non-paired helical filament pool in Alzheimer disease. J. Biol. Chem. 268, 24374–24384.

Lindwall, G., Cole, R.D., 1984. Phosphorylation affects the ability of tau protein to promote microtubule assembly. J. Biol. Chem. 259, 5301–5305.

Liu, F., Iqbal, K., Grundke-Iqbal, I., Hart, G.W., Gong, C.-X., 2004. O-GlcNAcylation regulates phosphorylation of tau: a mechanism involved in Alzheimer's disease. Proc. Natl. Acad. Sci. U. S. A 101, 10804–10809. https://doi.org/10.1073/pnas.0400348101.

MacKerell, A.D., Bashford, D., Bellott, M., Dunbrack, R.L., Evanseck, J.D., Field, M.J., Fischer, S., Gao, J., Guo, H., Ha, S., Joseph-McCarthy, D., Kuchnir, L., Kuczera, K., Lau, F.T.K., Mattos, C., Michnick, S., Ngo, T., Nguyen, D.T., Prodhom, B., Reiher, W. E., Roux, B., Schlenkrich, M., Smith, J.C., Stote, R., Straub, J., Watanabe, M., Wiórkiewicz-Kuczera, J., Yin, D., Karplus, M., 1998. All-atom empirical potential for molecular modeling and dynamics studies of proteins. J. Phys. Chem. B 102, 3586–3616. https://doi.org/10.1021/jp973084f.

Mandelkow, E.-M., Mandelkow, E., 1998. Tau in Alzheimer's disease. Trends Cell Biol. 8, 425–427.

Mandelkow, E., Song, Y.-H., Schweers, O., Marx, A., Mandelkow, E.-M., 1995. On the structure of microtubules, tau, and paired helical filaments. Neurobiol. Aging 16, 347–354. https://doi.org/10.1016/0197-4580(95)00026-B.

Mawal-Dewan, M., Henley, J., Van de Voorde, A., Trojanowski, J.Q., Lee, V.M., 1994. The phosphorylation state of tau in the developing rat brain is regulated by phosphoprotein phosphatases. J. Biol. Chem. 269, 30981–30987.

Mazanetz, M.P., Fischer, P.M., 2007. Untangling tau hyperphosphorylation in drug design for neurodegenerative diseases. Nat. Rev. Drug Discov. 6, 464.

McQuaid, M.J., Sun, H., Rigby, D., 2004. Development and validation of COMPASS force field parameters for molecules with aliphatic azide chains. J. Comput. Chem. 25, 61–71.

Mortazavi, B., Rabczuk, T., 2015. Multiscale modeling of heat conduction in graphene laminates. Carbon 85, 1–7.

Mortazavi, B., Yang, H., Mohebbi, F., Cuniberti, G., Rabczuk, T., 2017. Graphene or h-BN paraffin composite structures for the thermal management of Li-ion batteries: a multiscale investigation. Appl. Energy 202, 323–334.

Mulder, C., Verwey, N.A., van der Flier, W.M., Bouwman, F.H., Kok, A., van Elk, E.J., Scheltens, P., Blankenstein, M.A., 2010. Amyloid-β (1–42), total tau, and phosphorylated tau as cerebrospinal fluid biomarkers for the diagnosis of Alzheimer disease. Clin. Chem. 56, 248–253.

Noble, W., Planel, E., Zehr, C., Olm, V., Meyerson, J., Suleman, F., Gaynor, K., Wang, L., LaFrancois, J., Feinstein, B., 2005. Inhibition of glycogen synthase kinase-3 by lithium correlates with reduced tauopathy and degeneration in vivo. Proc. Natl. Acad. Sci. U. S. A. 102, 6990–6995.

Ono, T., Yamamoto, H., Tashima, K., Nakashima, H., Okumura, E., Yamada, K., Hisanaga, S.-I., Kishimoto, T., Miyakawa, T., Miyamoto, E., 1995. Dephosphorylation of abnormal sites of tau factor by protein phosphatases and its implication for Alzheimer's disease. Neurochem. Int. 26, 205–215.

Panda, D., Goode, B.L., Feinstein, S.C., Wilson, L., 1995. Kinetic stabilization of microtubule dynamics at steady state by tau and microtubule-binding domains of tau. Biochemistry 34, 11117–11127. https://doi.org/10.1021/bi00035a017.

Pearce, C.W., Young, P.G., 2014. On the pressure response in the brain due to short duration blunt impacts. PLoS One 9, e114292.

Pettersen, E.F., Goddard, T.D., Huang, C.C., Couch, G.S., Greenblatt, D.M., Meng, E.C., Ferrin, T.E., 2004. UCSF Chimera–a visualization system for exploratory research and analysis. J. Comput. Chem. 25, 1605–1612. https://doi.org/10.1002/jcc.20084.

Pickhardt, M., Bergen, M. v, Gazova, Z., Hascher, A., Biernat, J., Mandelkow, E.-M., Mandelkow, E., 2005. Screening for inhibitors of tau polymerization. Curr. Alzheimer Res. 2, 219–226.

Ravaglia, S., Bini, P., Sinforiani, E., Franciotta, D., Zardini, E., Tosca, P., Moglia, A., Costa, A., 2008. Cerebrospinal fluid levels of tau phosphorylated at threonine 181 in patients with Alzheimer's disease and vascular dementia. Neurol. Sci. 29, 417.

Rosenberg, K.J., Ross, J.L., Feinstein, H.E., Feinstein, S.C., Israelachvili, J., 2008. Complementary dimerization of microtubule-associated tau protein: implications for microtubule bundling and tau-mediated pathogenesis. Proc. Natl. Acad. Sci. U. S. A. 105, 7445–7450.

Rycroft, C., 2009. Voro++: a Three-Dimensional Voronoi Cell Library in C++. United States. https://doi.org/10.2172/946741.

Samsonov, A., Yu, J.-Z., Rasenick, M., Popov, S.V., 2004. Tau interaction with microtubules in vivo. J. Cell Sci. 117, 6129–6141. https://doi.org/10.1242/jcs.01531.

Santarella, R.A., Skiniotis, G., Goldie, K.N., Tittmann, P., Gross, H., Mandelkow, E.-M., Mandelkow, E., Hoenger, A., 2004. Surface-decoration of microtubules by human tau. J. Mol. Biol. 339, 539–553. https://doi.org/10.1016/j.jmb.2004.04.008.

Scott, C.W., Blowers, D.P., Barth, P.T., Lo, M.M.S., Salama, A.I., Caputo, C.B., 1991. Differences in the abilities of human tau isoforms to promote microtubule assembly. J. Neurosci. Res. 30, 154–162. https://doi.org/10.1002/jnr.490300116.

Selkoe, D.J., 1991. The molecular pathology of Alzheimer's disease. Neuron 6, 487–498.

Senftle, T.P., Hong, S., Islam, M.M., Kylasa, S.B., Zheng, Y., Shin, Y.K., Junkermeier, C., Engel-Herbert, R., Janik, M.J., Aktulga, H.M., 2016. The ReaxFF reactive force-field: development, applications and future directions. npj Comput. Mater. 2, 1–14.

Seubert, P., Mawal-Dewan, M., Barbour, R., Jakes, R., Goedert, M., Johnson, G.V.W., Litersky, J.M., Schenk, D., Lieberburg, I., Trojanowski, J.Q., 1995. Detection of phosphorylated Ser262 in fetal tau, adult tau, and paired helical filament tau. J. Biol. Chem. 270, 18917–18922.

Shultz, S.R., Wright, D.K., Zheng, P., Stuchbery, R., Liu, S.-J., Sashindranath, M., Medcalf, R.L., Johnston, L.A., Hovens, C.M., Jones, N.C., 2015. Sodium selenate reduces hyperphosphorylated tau and improves outcomes after traumatic brain injury. Brain 138, 1297–1313.

Sjögren, M., Davidsson, P., Tullberg, M., Minthon, L., Wallin, A., Wikkelso, C., Granérus, A.-K., Vanderstichele, H., Vanmechelen, E., Blennow, K., 2001. Both total and phosphorylated tau are increased in Alzheimer's disease. J. Neurol. Neurosurg. Psychiatry 70, 624–630.

Sochocka, M., Ochnik, M., Sobczyński, M., Siemieniec, I., Orzechowska, B., Naporowski, P., Leszek, J., 2019. New therapeutic targeting of Alzheimer's disease with the potential use of proline-rich polypeptide complex to modulate an innate immune response-preliminary study. J. Neuroinflammation 16, 137.

Stukowski, A., 2010. Visualization and analysis of atomistic simulation data with OVITO–the Open Visualization Tool. Model. Simulat. Mater. Sci. Eng. 18, 015012 https://doi.org/10.1088/0965-0393/18/1/015012.

Tang-Schomer, Min D., Patel, Ankur R., Baas, Peter W., Smith, Douglas H., 2009. Mechanical breaking of microtubules in axons during dynamic stretch injury underlies delayed elasticity, microtubule disassembly, and axon degeneration. FASEB J. 24, 1401–1410. https://doi.org/10.1096/fj.09-142844.

Trinczek, B., Biernat, J., Baumann, K., Mandelkow, E.M., Mandelkow, E., 1995. Domains of tau protein, differential phosphorylation, and dynamic instability of microtubules. Mol. Biol. Cell 6, 1887–1902. https://doi.org/10.1091/mbc.6.12.1887.

Uversky, V.N., 2010. Targeting intrinsically disordered proteins in neurodegenerative and protein dysfunction diseases: another illustration of the D2 concept. Expert Rev. Proteomics 7, 543–564.

Vanmechelen, E., Vanderstichele, H., Davidsson, P., Van Kerschaver, E., Van Der Perre, B., Sjögren, M., Andreasen, N., Blennow, K., 2000. Quantification of tau phosphorylated at threonine 181 in human cerebrospinal fluid: a sandwich ELISA with a synthetic phosphopeptide for standardization. Neurosci. Lett. 285, 49–52.

Watanabe, A., Hasegawa, M., Suzuki, M., Takio, K., Morishima-Kawashima, M., Titani, K., Arai, T., Kosik, K.S., Ihara, Y., 1993. In vivo phosphorylation sites in fetal and adult rat tau. J. Biol. Chem. 268, 25712–25717.

Wells, D.B., Aksimentiev, A., 2010. Mechanical properties of a complete microtubule revealed through molecular dynamics simulation. Biophys. J. 99, 629–637.

Wu, Y.-T., Adnan, A., 2018. Damage and failure of axonal microtubule under extreme high strain rate: an in-silico molecular dynamics study. Sci. Rep. 8, 12260.

Yuzwa, S.A., Macauley, M.S., Heinonen, J.E., Shan, X., Dennis, R.J., He, Y., Whitworth, G.E., Stubbs, K.A., McEachern, E.J., Davies, G.J., Vocadlo, D.J., 2008. A potent mechanism-inspired O-GlcNAcase inhibitor that blocks phosphorylation of tau in vivo. Nat. Chem. Biol. 4, 483.

Zhang, Y., 2008. I-TASSER server for protein 3D structure prediction. BMC Bioinf. 9, 40.